Prospects for $B^0_{(s)} \to \pi^0\pi^0, \eta\eta$ measurement and CKM angle α determination via $B \to \pi\pi$ modes at CEPC (Tera-Z)

[JHEP12(2022)135]

Yuexin Wang, Sébastien, Olivier, Lingfeng Li,
Manqi Ruan, Shanzhen Chen, Yongfeng Zhu

Status of $B^0_{(s)} \to \pi^0\pi^0, \eta\eta$

Experimental and theoretical branching ratios (in units of 10^{-6})

Channel	DATA	SCET [1]	QCDF	pQCD
$B^0 \to \pi^0\pi^0$	1.59 ± 0.26 [2]	$0.84 \pm 0.29 \pm 0.30 \pm 0.19$	$0.30^{+0.46}_{-0.26}$	$0.24^{+0.09}_{-0.07}$
$B^0_s \to \pi^0\pi^0$	< 210 [3]	-	$0.13^{+0.05}_{-0.05}$ [10]	$0.21^{+0.10}_{-0.09}$ [5] $0.28^{+0.08+0.04+0.01}_{-0.07-0.05-0.00}$ [4]
$B^0 \to \eta\eta$	< 1 [6]	$0.69 \pm 0.38 \pm 0.13 \pm 0.58$ $1.0 \pm 0.4 \pm 0.3 \pm 1.4$	$0.32^{+0.13+0.07}_{-0.05-0.06}$ [7] $0.16^{+0.03+0.43+0.09+0.10}_{-0.03-0.18-0.03-0.05}$ [8]	0.067 [9]
$B^0_s \to \eta\eta$	< 1500 [3]	$7.1 \pm 6.4 \pm 0.2 \pm 0.8$ $6.4 \pm 6.3 \pm 0.1 \pm 0.7$	$10.9^{+6.3+5.7}_{-4.0-4.2}$ [10]	$10.4^{+4.9}_{-3.4}$ [5]

➢ Only $B^0 \to \pi^0\pi^0$ has been observed experimentally
➢ $B^0 \to \pi^0\pi^0$
  ➢ Puzzle: discrepancy between experimental and theoretical BR
  ➢ Necessary channel to determine CKM angle α
➢ Charmless two-body hadronic B-meson decay
  ➢ experimentally clean
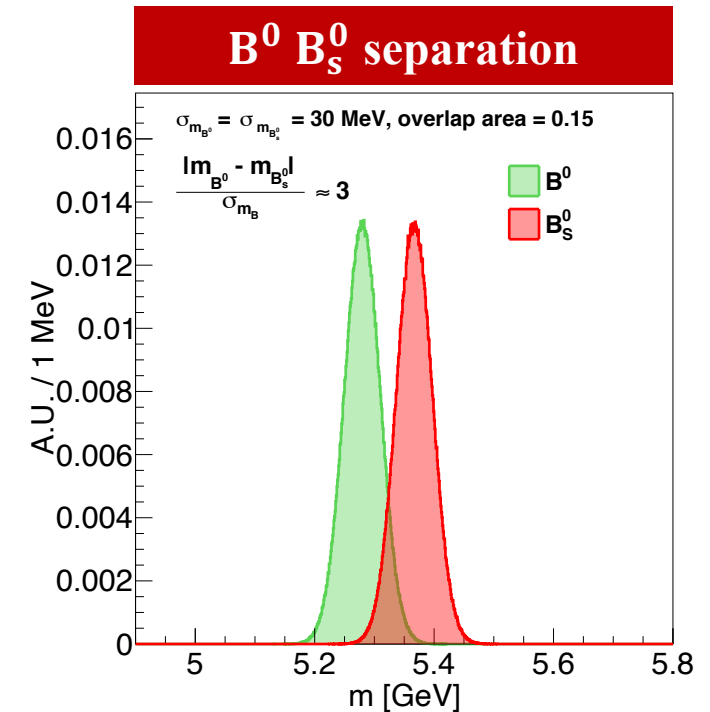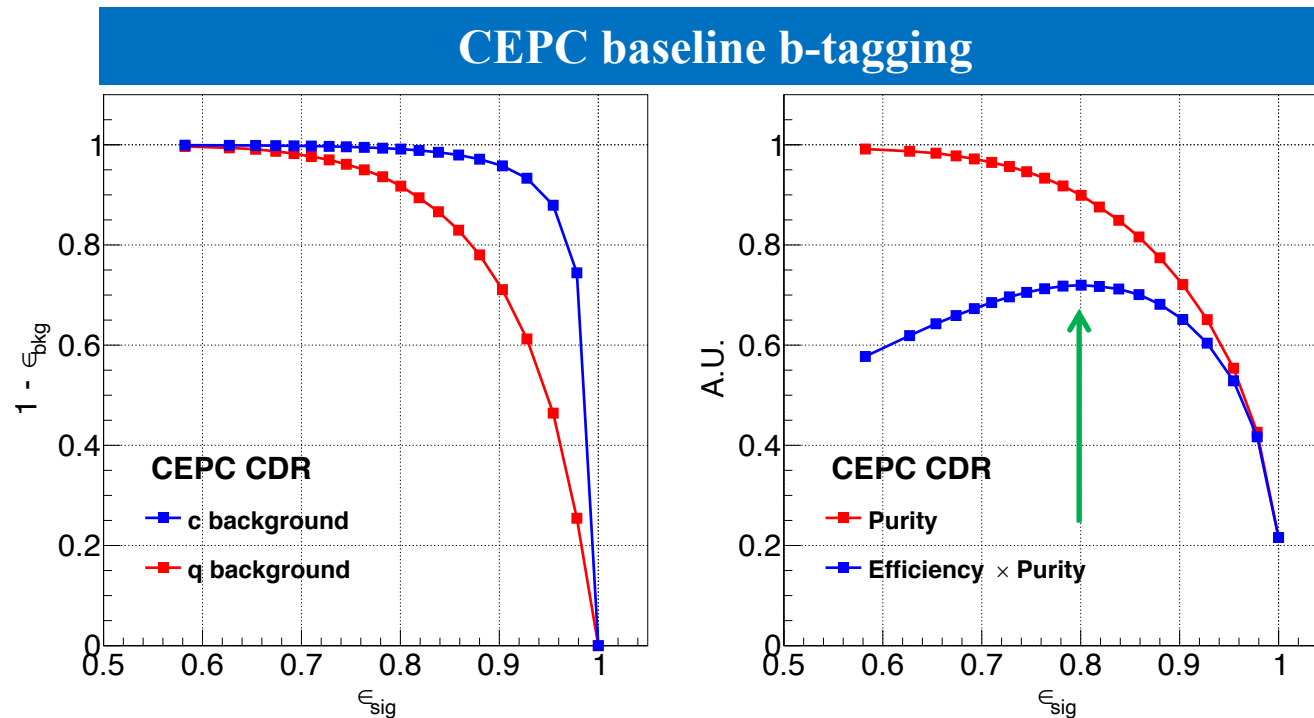 ➢ hadron physics, even new physics

Advantage of CEPC

➢ Tera-Z factory
  ➢ Massive various b-hadrons
    $\sim 10^{11}\ B^0\ \&\ \sim 10^{10}\ B_s^0$
  ➢ Larger boost of b-hadrons than Belle II → more precise vertex reconstruction
➢ Lepton collider
  ➢ Cleaner collision environment and much lower background level
  ➢ Benefit neutral final states reconstruction

| b-hadrons	Belle II	LHCb (300 fb^{-1})	Tera-Z
$B^0,\ \bar{B}^0$	5.4×10^{10} (50 ab^{-1} on $\Upsilon(4S)$)	3×10^{13}	1.2×10^{11}
$B^\pm$	5.7×10^{10} (50 ab^{-1} on $\Upsilon(4S)$)	3×10^{13}	1.2×10^{11}
$B_s^0,\ \bar{B}_s^0$	6.0×10^8 (5 ab^{-1} on $\Upsilon(5S)$)	1×10^{13}	3.1×10^{10}
$B_c^\pm$	-	1×10^{11}	1.8×10^8
$\Lambda_b^0,\ \bar{\Lambda}_b^0$	-	2×10^{13}	2.5×10^{10}

Key detector performance

- Fast simulation strategy
- b-jet tagging
  - CEPC baseline: $\varepsilon \sim 80\%$, $p \sim 90\%$
- ECAL performance
  - Only focus on di-photon decay of π^0 and η
  - B mass resolution: $\sigma_{m_B} \sim 30\text{MeV} \rightarrow 3\sigma$ separation between B^0 and B_s^0
  - EM resolution: improve the baseline $17\%/\sqrt{E} \oplus 1\%$ to $3\%/\sqrt{E} \oplus 0.3\%$
    - e.g. Homogeneous crystal ECAL design of CEPC 4th concept detector

CEPC baseline b-tagging

CEPC CDR
- c background
- q background

CEPC CDR
- Purity
- Efficiency × Purity

B^0 B_s^0 separation

$\sigma_{m_{B^0}} = \sigma_{m_{B_s^0}} = 30$ MeV, overlap area = 0.15

$$\frac{|m_{B^0} - m_{B_s^0}|}{\sigma_{m_B}} \approx 3$$

- B^0
- B_s^0

Event selection of $B^0_{(s)} \to \pi^0\pi^0$

Selection chain	$B^0 \to \pi^0\pi^0 \to 4\gamma$	$B^0_s \to \pi^0\pi^0 \to 4\gamma$	$u\bar{u}+d\bar{d}+s\bar{s}$	$c\bar{c}$	$b\bar{b}$	$\sqrt{S+B}/S$
Yield at Tera-Z	191113	8948	4.29×10^{11} (61.21%)	1.20×10^{11} (17.19%)	1.51×10^{11} (21.60%)	
b-tagging	152890	7159	3.64×10^{9} (2.70%)	9.94×10^{9} (7.38%)	1.21×10^{11} (89.92%)	
$\pi^0 \to \gamma\gamma$	148213	6953	3.61×10^{9}	9.91×10^{9}	1.21×10^{11}	
Lower $E_{\pi^0} > 6$ GeV	92407	4391	8.44×10^{8}	1.60×10^{9}	1.31×10^{10}	
Higher $E_{\pi^0} > 14$ GeV	87355	4142	3.08×10^{8}	3.15×10^{8}	1.91×10^{9}	
$E_{\pi^0\pi^0} > 22$ GeV	87073	4127	2.90×10^{8}	2.82×10^{8}	1.66×10^{9}	
$\theta_{\pi^0\pi^0} < 23°$	77970	3636	1.19×10^{8}	1.02×10^{8}	6.04×10^{8}	
$m_{\pi^0\pi^0} \in (5.212, 5.347)$ GeV	75859	933	5472	1622	8673	0.40% $\pm$ 0.01%
$m_{\pi^0\pi^0} \in (5.336, 5.397)$ GeV	2831	2545	2424	473	2248	4.0% $\pm$ 0.6%
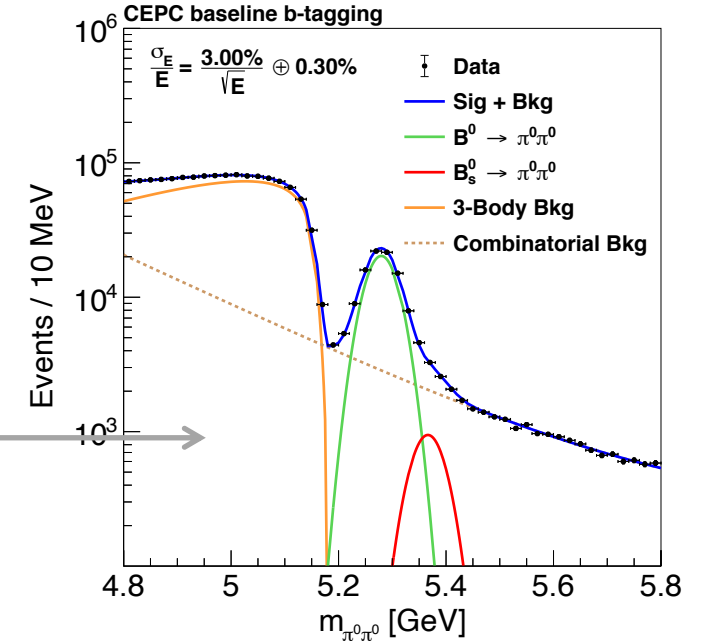
> Cut-based event selection (on energy and angular distributions of π^0 pairs)
>> Signal efficiency ~ 40%
>> Background suppression ~ 3 orders of magnitude
> Optimize mass window → minimize relative accuracy $\sqrt{S+B}/S$
>> ~ 7.5×10^4 $B^0 \to \pi^0\pi^0$, relative accuracy ~ 0.4%
>> ~ 2.5×10^3 $B^0_s \to \pi^0\pi^0$, relative accuracy ~ 4.0%

Event selection of $B^0_{(s)} \to \eta\eta$

Selection chain	$B^0 \to \eta\eta \to 4\gamma$	$B^0_s \to \eta\eta \to 4\gamma$	$u\bar{u}+d\bar{d}+s\bar{s}$	$c\bar{c}$	$b\bar{b}$	$\sqrt{S+B}/S$
Yield at Tera-Z	1912	47437	4.29×10^{11}	1.20×10^{11}	1.51×10^{11}	
b-tagging	1529	37950	3.64×10^{9}	9.94×10^{9}	1.21×10^{11}	
$\eta \to \gamma\gamma$	1000	25820	2.13×10^{8}	5.60×10^{8}	9.41×10^{9}	
$E_{\eta\eta} > 20$ GeV	934	24158	1.39×10^{7}	1.09×10^{7}	9.46×10^{7}	
$\theta_{\eta\eta} < 30°$	814	21135	6.76×10^{6}	5.68×10^{6}	5.17×10^{7}	
$m_{\eta\eta} \in (5.233, 5.326)$ GeV	693	2103	2328	676	8030	17% $\pm$ 2%
$m_{\eta\eta} \in (5.310, 5.423)$ GeV	155	19208	2184	1014	7388	0.90% $\pm$ 0.05%
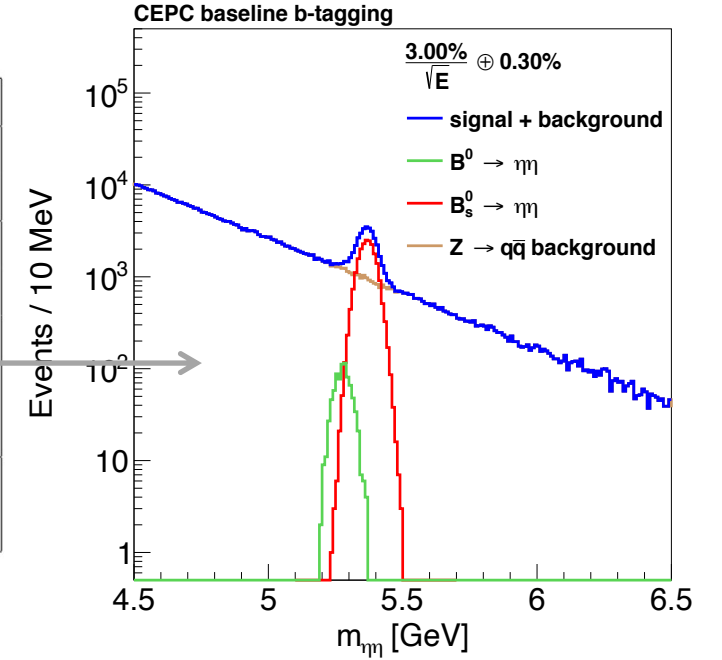
CEPC baseline b-tagging

$\frac{3.00\%}{\sqrt{E}} \oplus 0.30\%$

- signal + background
- $B^0 \to \eta\eta$
- $B^0_s \to \eta\eta$
- $Z \to q\bar{q}$ background

➢ Cut-based event selection (on energy and angular distributions of η pairs)
  ➢ Signal efficiency ~ 45%
  ➢ Background suppression ~ 5 orders of magnitude
➢ Optimize mass window → minimize relative accuracy $\sqrt{S+B}$/S
  ➢ ~ 700 $B^0 \to \eta\eta$, relative accuracy ~ 17%
  ➢ ~ 2×10^4 $B^0_s \to \eta\eta$, relative accuracy ~ 0.9%

Other effects

➢ Photon conversion
    ➢ Central region ~5-10%, Forward region ~25%, ~80% can be recovered
    ➢ Average conversion rate ~3% (each photon)
        → 12% efficiency loss of $B^0_{(s)} \to \pi^0\pi^0, \eta\eta$

➢ Photon separation (especially di-photon merging)
    ➢ 2cm → 80% separation efficiency (CEPC baseline, 5GeV γ)
    ➢ 2cm → 10 mrad angular separation (ECAL R_{inner}=2m)
    ➢ Only energetic π^0 suffers
        → 10% efficiency loss of $B^0_{(s)} \to \pi^0\pi^0$
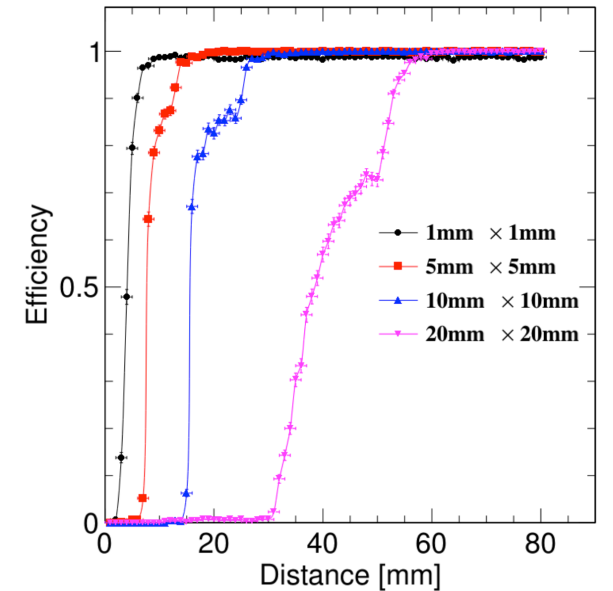
Final realistic results

Channels	$B^0 \to \pi^0\pi^0$	$B^0_s \to \pi^0\pi^0$	$B^0 \to \eta\eta$	$B^0_s \to \eta\eta$
Signal yield	60000	2000	600	17500
Accuracy	0.45%	4.5%	18%	0.95%
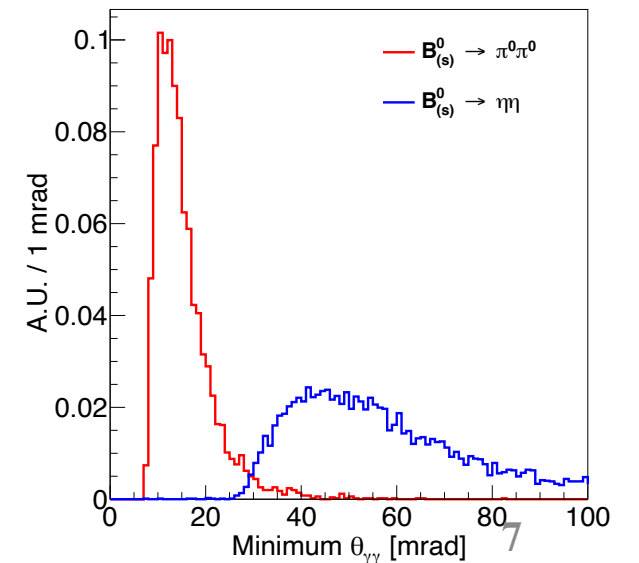
Determination of CKM angle α

- CKM matrix: quark mixing, CP violation
- B^0 decay related triangle relation

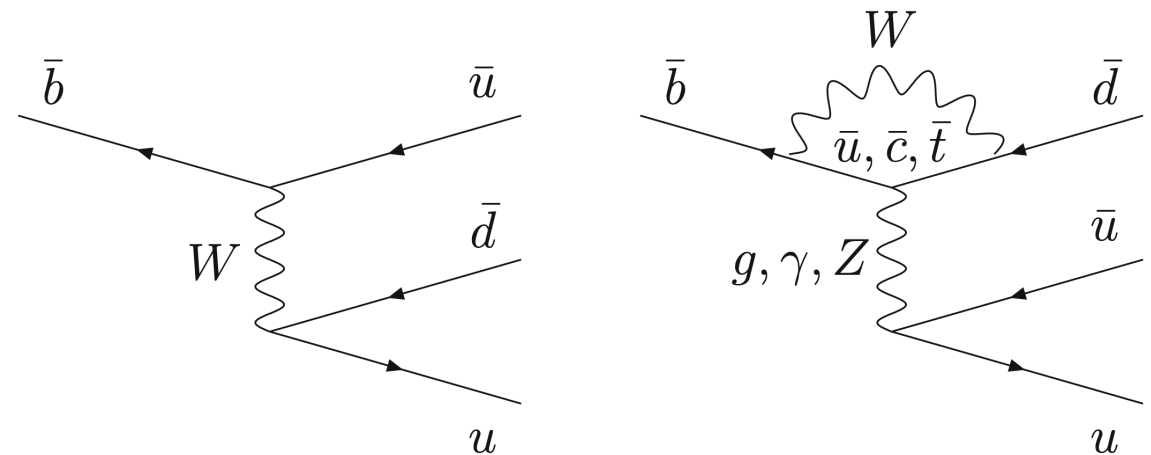$$V_{ub}V_{ud}^* + V_{cb}V_{cd}^* + V_{tb}V_{td}^* = 0,$$
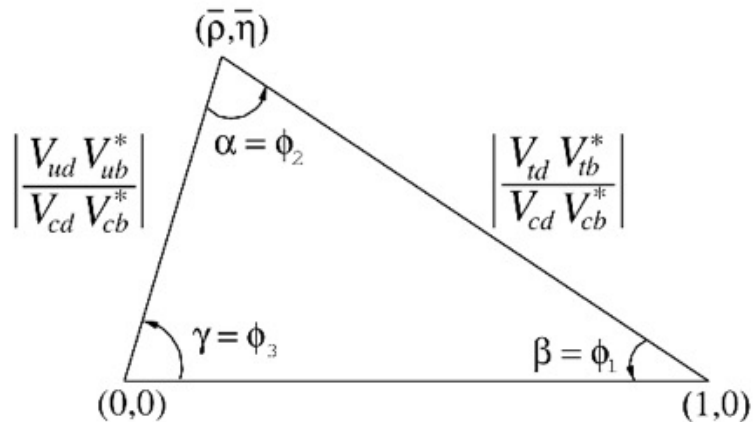
Figure 12.1: Sketch of the unitarity triangle.

$$\beta = \phi_1 = \arg\left(-\frac{V_{cd}V_{cb}^*}{V_{td}V_{tb}^*}\right),$$

$$\alpha = \phi_2 = \arg\left(-\frac{V_{td}V_{tb}^*}{V_{ud}V_{ub}^*}\right),$$

$$\gamma = \phi_3 = \arg\left(-\frac{V_{ud}V_{ub}^*}{V_{cd}V_{cb}^*}\right).$$

- α determination via weak transition b → uud
  - Commonly used decay modes
    - $B \to \rho\rho, \pi\pi, \rho\pi$
  - Both tree and penguin diagrams
  - Penguin contribution is non-negligible
  - Using isospin conservation to deal with penguin pollution

Determination of CKM angle α

Isospin analysis of $B \to \pi\pi$: $B^0 \to \pi^0\pi^0, \pi^+\pi^-, B^+ \to \pi^+\pi^0$

➢ 3 amplitudes can be parameterized by 12 real parameters (complex tree and penguin contributions)

➢ 6 parameters can be further eliminated by:

    ➢ 2 complex isospin relations (4 real constraints) $\longrightarrow$

$$A^{+0} = \frac{1}{\sqrt{2}} A^{+-} + A^{00}$$

    ➢ absence of penguin contribution to $B^+ \to \pi^+\pi^0$ (2 real constraints)

➢ Remain only 6 degrees of freedom!

$$\bar{A}^{-0} = \frac{1}{\sqrt{2}} \bar{A}^{+-} + \bar{A}^{00}$$

➢ From experimental side

    ➢ 6 observables are available to constrain the 6D parameter space

        ➢ $\mathcal{B}^{ij}$: branching ratio

        ➢ $\mathcal{C}^{ij}$: direct CP asymmetry in decay

        ➢ $\mathcal{S}^{ij}$: B^0-$\bar{B}^0$ mixing induced CP asymmetry

$$\frac{1}{\tau_{B^{i+j}}} \mathcal{B}^{ij} = \frac{|A^{ij}|^2 + |\bar{A}^{ij}|^2}{2},$$

$$\mathcal{C}^{ij} = \frac{|A^{ij}|^2 - |\bar{A}^{ij}|^2}{|A^{ij}|^2 + |\bar{A}^{ij}|^2},$$

$$\mathcal{S}^{ij} = \frac{2\mathcal{I}m(\bar{A}^{ij} A^{ij*})}{|A^{ij}|^2 + |\bar{A}^{ij}|^2},$$

Current input observables to determine α

Parameters	World average [30]	Belle (0.8 ab^{-1})	Belle II (50 ab^{-1}) [18]	LHCb
$\mathcal{B}^{00}$ ($\times 10^{-6}$)	1.59 $\pm$ 0.26 (16%)	1.31 [31] $\pm$ 0.19 (14.5%) $\pm$ 0.19	1.31 $\pm$ 0.03 (2.3%) $\pm$ 0.03	-
$\mathcal{B}^{+0}$ ($\times 10^{-6}$)	5.5 $\pm$ 0.4 (7.3%)	5.86 [59] $\pm$ 0.26 (4.4%) $\pm$ 0.38	5.86 $\pm$ 0.03 (0.6%) $\pm$ 0.09	-
$\mathcal{B}^{+-}$ ($\times 10^{-6}$)	5.12 $\pm$ 0.19 (3.7%)	5.04 [59] $\pm$ 0.21 (4.2%) $\pm$ 0.18	5.04 $\pm$ 0.03 (0.6%) $\pm$ 0.08	-
C_{CP}^{00}	-0.33 $\pm$ 0.22	-0.14 [31] $\pm$ 0.36 $\pm$ 0.10	-0.14 $\pm$ 0.03 $\pm$ 0.01	-
C_{CP}^{+-}	-0.314 $\pm$ 0.030	-0.33 [60] $\pm$ 0.06 $\pm$ 0.03	-0.33 $\pm$ 0.01 $\pm$ 0.03	-0.34 $\pm$ 0.06 $\pm$ 0.01 [61] (7 & 8 TeV, 3.0 fb^{-1}) -0.311 $\pm$ 0.045 $\pm$ 0.015 [62] (13 TeV, 1.9 fb^{-1}) $\pm$ 0.004 (stat. only) [19] (Run 1–6, 300 fb^{-1})
S_{CP}^{+-}	-0.670 $\pm$ 0.030	-0.64 [60] $\pm$ 0.08 $\pm$ 0.03	-0.64 $\pm$ 0.01 $\pm$ 0.01	-0.63 $\pm$ 0.05 $\pm$ 0.01 [61] (7 & 8 TeV, 3.0 fb^{-1}) -0.706 $\pm$ 0.042 $\pm$ 0.013 [62] (13 TeV, 1.9 fb^{-1}) $\pm$ 0.004 (stat. only) [19] (Run 1–6, 300 fb^{-1})

➢ No S_{CP}^{00} (mixing induced CP asymmetry) in current data
    ➢ Lack of vertex information in $B^0 \to \pi^0 \pi^0 \to 4\gamma$ to perform time-dependent measurement
    ➢ Lead to mirror solutions in α

Complementarity between Z- and B-factory

➤ Time-integrated CP measurements at Z- and B-factories are quite different but complementary!

  ➤ Z-factory (B from bb pairs, incoherently), $t \in [0, \infty)$, $a_{CP} = C + xS$.

  ➤ B-factory ($\Upsilon \rightarrow BB$, coherently), $t \rightarrow \Delta t \in (-\infty, +\infty)$, $a_{CP} = C$.

➤ An alternative way to extract S_{CP}^{00} by combining Z- and B-factories

$|q_d/p_d| \simeq 1$ [26]. The time-dependent decay rates become [42–44]:

$$\Gamma_{B^0/\bar{B}^0 \rightarrow f_{CP}}(t) \propto \boxed{e^{-\Gamma_d t}} \left[1 \pm C_{f_{CP}} \cos(\Delta m_d t) \mp S_{f_{CP}} \boxed{\sin(\Delta m_d t)} \right].$$

$$\boxed{e^{-\Gamma|\Delta t|}}$$
even

odd

$$C_{f_{CP}} \equiv \frac{1 - |\lambda_{f_{CP}}|^2}{1 + |\lambda_{f_{CP}}|^2}, \quad S_{f_{CP}} \equiv \frac{2\text{Im}\lambda_{f_{CP}}}{1 + |\lambda_{f_{CP}}|^2}, \quad \lambda_{f_{CP}} \equiv \frac{q_d}{p_d} \frac{\bar{\mathcal{A}}_{f_{CP}}}{\mathcal{A}_{f_{CP}}},$$

This leads to the definition of the measured time-dependent CP asymmetry:

$$a_{f_{CP}}(t) \equiv \frac{\Gamma_{\bar{B} \rightarrow f_{CP}}(t) - \Gamma_{B \rightarrow f_{CP}}(t)}{\Gamma_{\bar{B} \rightarrow f_{CP}}(t) + \Gamma_{B \rightarrow f_{CP}}(t)} \simeq -C_{f_{CP}} \cos(\Delta m_d t) + S_{f_{CP}} \sin(\Delta m_d t),$$

and the time-integrated CP asymmetry:

$$\int_{-\infty}^{\infty}$$

$$a_{f_{CP}} \equiv \frac{\int_0^\infty \Gamma_{\bar{B} \rightarrow f_{CP}}(t) - \Gamma_{B \rightarrow f_{CP}}(t)dt}{\int_0^\infty \Gamma_{\bar{B} \rightarrow f_{CP}}(t) + \Gamma_{B \rightarrow f_{CP}}(t)dt} \simeq \frac{1}{1 + (\Delta m_d/\Gamma_d)^2} \left(-C_{f_{CP}} + S_{f_{CP}} \frac{\Delta m_d}{\Gamma_d} \right).$$

**linear combination**

11

α determination via $B \to \pi\,\pi$

- Extract α from $B \to \pi\,\pi$ modes
  - 3 channels: $B^0 \to \pi^0\pi^0, \pi^+\pi^-, B^+ \to \pi^+\pi^0$
  - Input observables: BR & CP asymmetries
- Uncertainty estimation (statistical only)

$$\frac{\sigma_{\mathcal{B}}}{\mathcal{B}} \simeq \frac{1}{\sqrt{N_{\text{eff}}}} \equiv \frac{1}{\sqrt{\text{Yield} \times \epsilon \times p}}$$

$$\sigma_{a_{CP}^{00}} \simeq \frac{1}{(1 - 2\chi_d)\sqrt{N_{\text{eff}} \times \epsilon_{\text{eff}}}} \quad \text{(time-integrated)}$$

$$\sigma_{S_{CP}^{+-}} \simeq \sigma_{C_{CP}^{+-}} \simeq \frac{1}{\sqrt{N_{\text{eff}} \times \epsilon_{\text{eff}}}} \quad \text{(time-dependent)}$$

- Key parameters in CP measurements:
  - b-charge tagging (B^0 or $\bar{B}^0$):
    - tagging efficiency, ϵ_{tag}
    - wrong tagging fraction, ω
    - effective tagging efficiency (power), ϵ_{eff}
    - we use $\epsilon_{\text{eff}} \equiv \epsilon_{\text{tag}}(1 - 2\omega)^2 \in [15,25]\%$
  - B^0-$\bar{B}^0$ mixing: $\chi_d = 0.1858 \pm 0.0011$
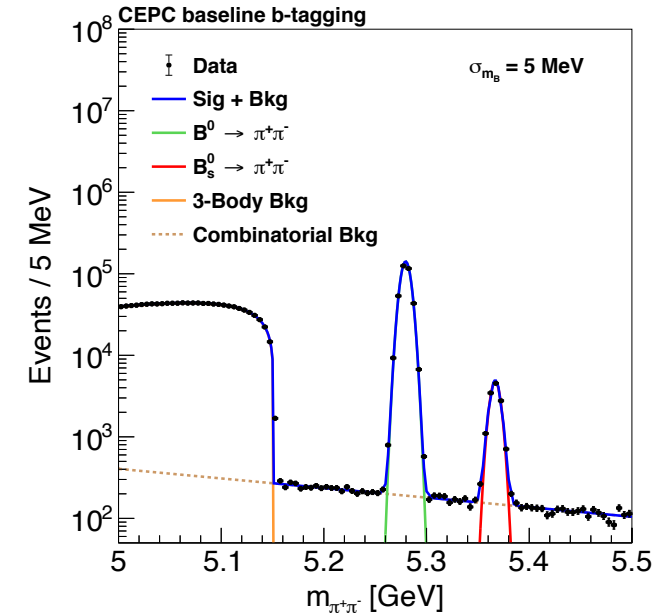
Parameters	Tera-Z Projection
$\sigma_{\mathcal{B}^{00}}/\mathcal{B}^{00}$	0.45%
$\sigma_{\mathcal{B}^{+0}}/\mathcal{B}^{+0}$	0.19%
$\sigma_{\mathcal{B}^{+-}}/\mathcal{B}^{+-}$	0.18%
$\sigma_{a_{CP}^{00}}$	$\pm$ (0.014–0.018)
$\sigma_{C_{CP}^{+-}}$	$\pm$ (0.004–0.005)
$\sigma_{S_{CP}^{+-}}$	$\pm$ (0.004–0.005)

Impact on CKM angle α determination

- CKM global fit (by Sébastien & Olivier, CKMfitter group)
  - Uncertainties rescaled to Tera-Z projections
- Scenario 1: only improve $B^0 \to \pi^0\pi^0$ to Tera-Z projection
  - Main improvement comes from a_{CP}^{00}
  - Some mirror solutions removed with $a_{CP}^{00} = C + xS$ at Tera-Z
  - Final precision of α: 2~3° (with additional C_{WA}^{00} from B-factories)

$$\text{WA}: \alpha(\pi\pi) = (93.0 \pm 13.6)° \to \text{Tera-}Z \text{ scenario } 1: \alpha(\pi\pi) = (82.6^{+3.5}_{-2.5} \cup 92.0^{+1.4}_{-2.0})°$$
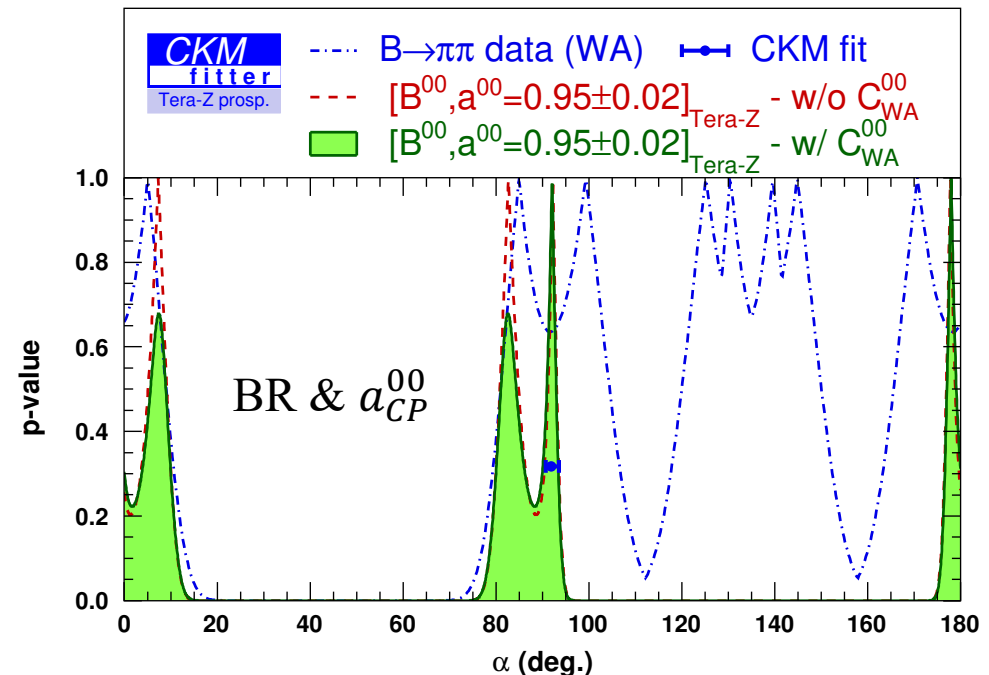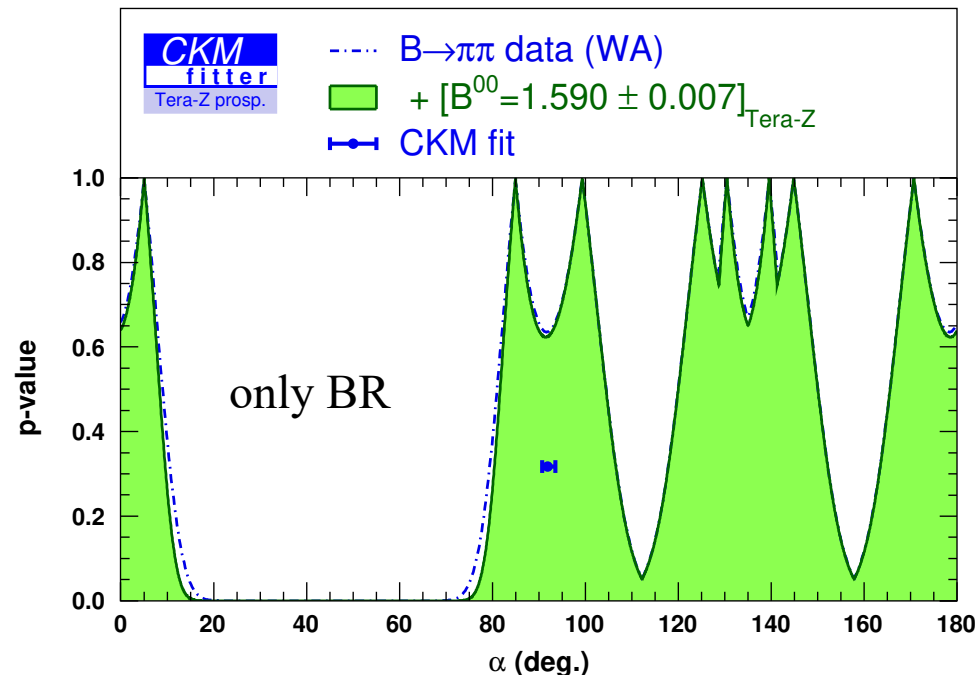
Impact on CKM angle α determination

- Scenario 2: improve all three $B \to \pi\pi$ modes to Tera-Z projection
  - a_{CP}^{00} and C_{CP}^{00} are central in this improvement
  - Final precision of α:

$$\text{Tera-}Z \text{ scenario } 2 : \alpha(\pi\pi) = (91.8 \pm 0.4)^\circ$$

  - Even better than:
    - Current world average combining $\rho\rho, \pi\pi, \rho\pi$ data $\sim 1.4^\circ$
    - Theoretical systematic uncertainties (isospin related) $\sim$ 1-2°, need reevaluation
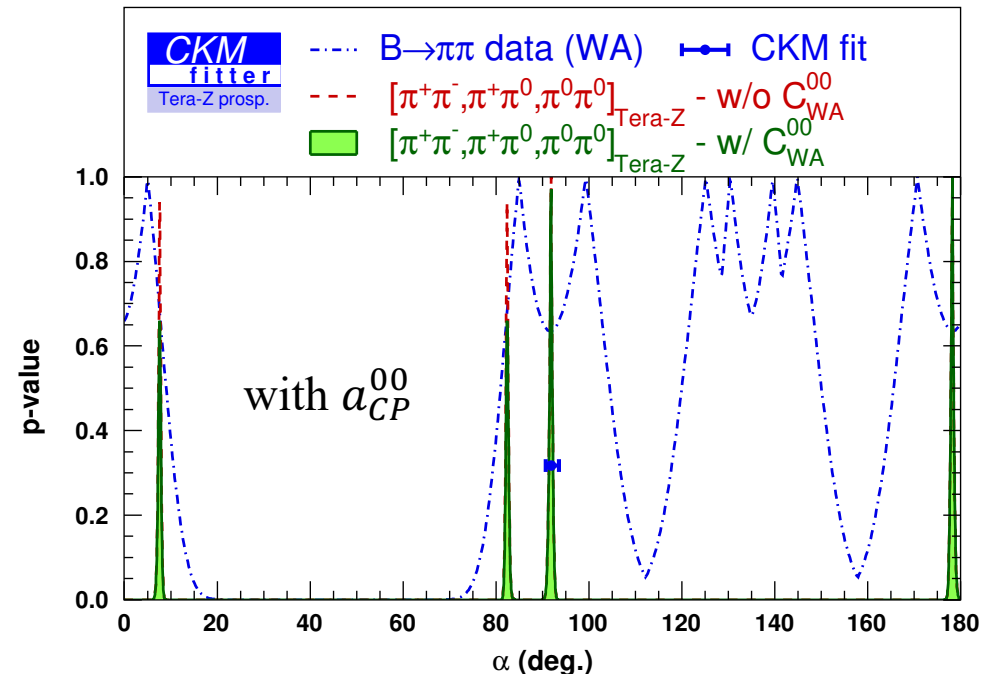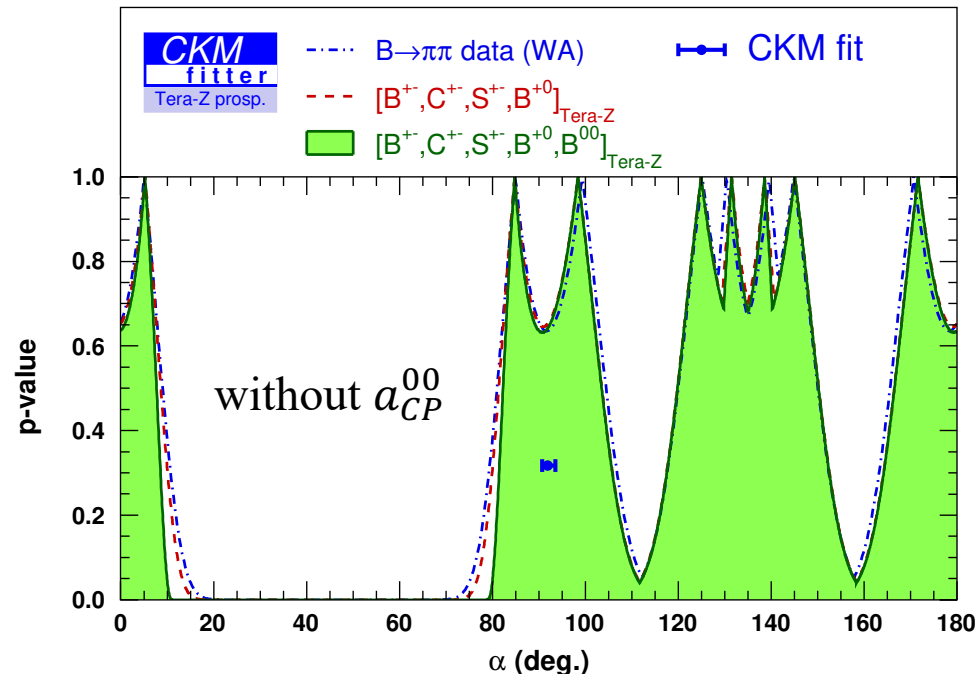
Other prospects for α measurement

> Direct extraction of $S_{\pi\pi}^{00}$ via time-dependent analysis of $B^0 \to \pi^0\pi^0$
>> Using $\pi^0 \to e^+e^-\gamma$ Dalitz decay or photon conversion events
>> CEPC advantage
>>> Larger boost of B meson
>>> Decent vertex reconstruction
>>> B decay lifetime resolution ~15 fs

> $B \to \rho\rho$, more precise than $B \to \pi\pi$ modes
>> Larger branching ratios than $B \to \pi\pi$
>> $B^0 \to \rho^0\rho^0$ enjoys the charged final state $\rho^0 \to \pi^+\pi^-$
>>> Much better charged particle reconstruction performance than neutral particle
>>> $S_{\rho\rho}^{00}$ is available to reduce the mirror solutions in α

Summary

- Neutral charmless B-meson decays: $B^0_{(s)} \to \pi^0\pi^0, \eta\eta$
  - Fast simulation: key detector performance modeling
    - CEPC baseline b-tagging: $\varepsilon \sim 80\%$, $p \sim 90\%$
    - EM resolution: $3\%/\sqrt{E} \oplus 0.3\%$ ($\sigma_{m_B} \sim 30\text{MeV}$)
    - Other effects: photon conversion & separation
  - Anticipated accuracy at Tera-Z $\longrightarrow$

Channels	$B^0 \to \pi^0\pi^0$	$B^0_s \to \pi^0\pi^0$	$B^0 \to \eta\eta$	$B^0_s \to \eta\eta$
Signal yield	60000	2000	600	17500
Accuracy	0.45%	4.5%	18%	0.95%

- CKM angle α determination using $B \to \pi\pi$ mode
  - Complementarity between Z- and B-factory in
    - extracting S^{00}_{CP}
    - reducing mirror solutions in α
  - Anticipated precisions of $B \to \pi\pi$ BR & CP asymmetries $\longrightarrow$
  - CKM global fit results
    - Only improve $B^0 \to \pi^0\pi^0$: $\sigma(\alpha) \approx 2{\sim}3°$
    - Improve all three $B \to \pi\pi$: $\sigma(\alpha) \approx 0.4°$
  - Prospects
    - Reevaluation of theoretical systematic uncertainties
    - Direct extraction of $S^{00}_{\pi\pi}$ via π^0 Dalitz decay or photon conversion
    - More precise measurement of $B \to \rho\rho$

Parameters	Tera-Z Projection
$\sigma_{\mathcal{B}^{00}}/\mathcal{B}^{00}$	0.45%
$\sigma_{\mathcal{B}^{+0}}/\mathcal{B}^{+0}$	0.19%
$\sigma_{\mathcal{B}^{+-}}/\mathcal{B}^{+-}$	0.18%
$\sigma_{a^{00}_{CP}}$	$\pm(0.014\text{–}0.018)$
$\sigma_{C^{+-}_{CP}}$	$\pm(0.004\text{–}0.005)$
$\sigma_{S^{+-}_{CP}}$	$\pm(0.004\text{–}0.005)$

Thank you for your attention!

Reconstruction performance of π^0 and η

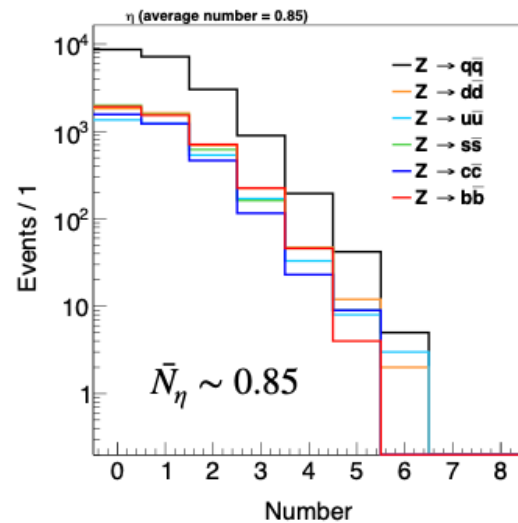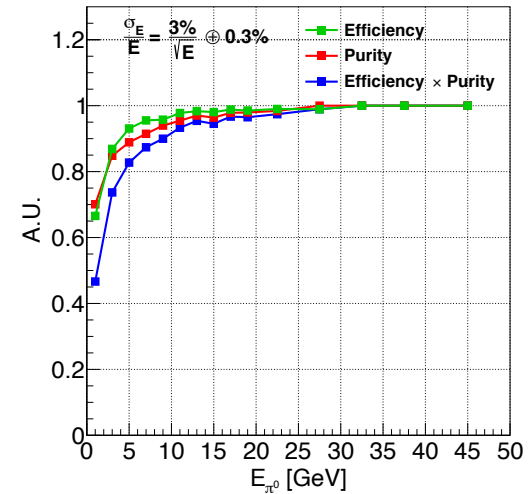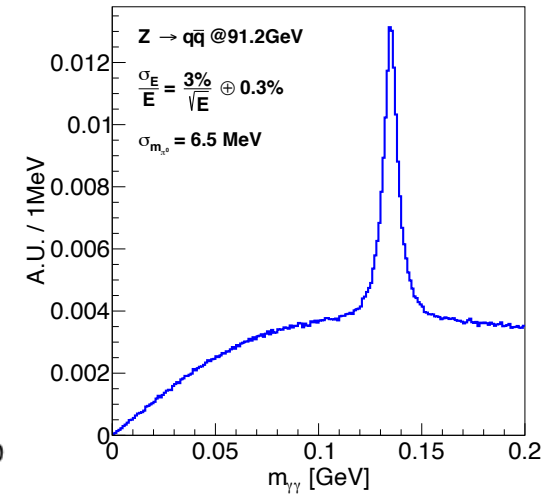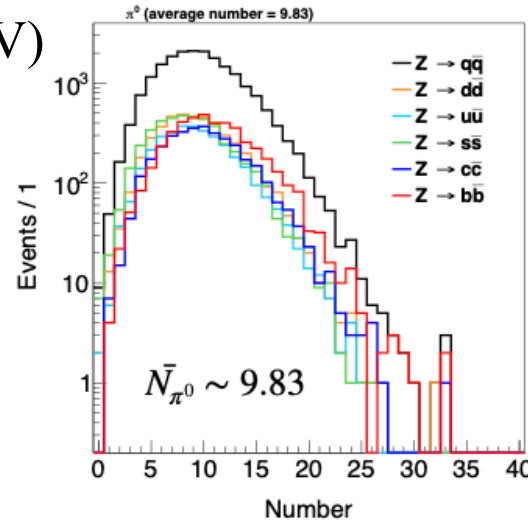> Inclusive π^0 and η in $Z \to q\bar{q}$ (91.2 GeV)
>> $\bar{N}_{\pi^0} \gg \bar{N}_\eta$
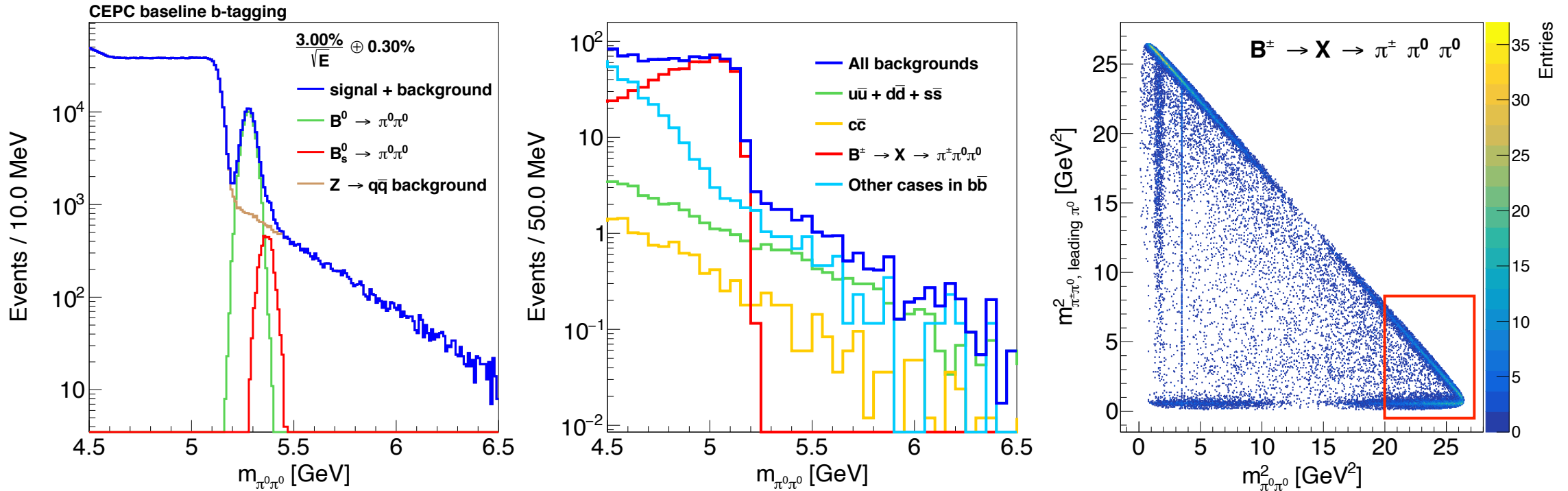>> prioritize π^0 reconstruction, use remaining γ to reconstruct η

> Optimal $\epsilon \times p$ vs $E_{\pi^0, \eta}$
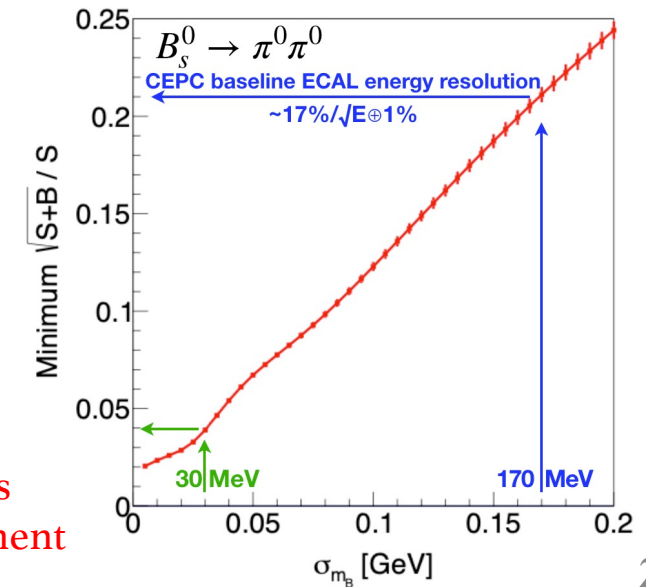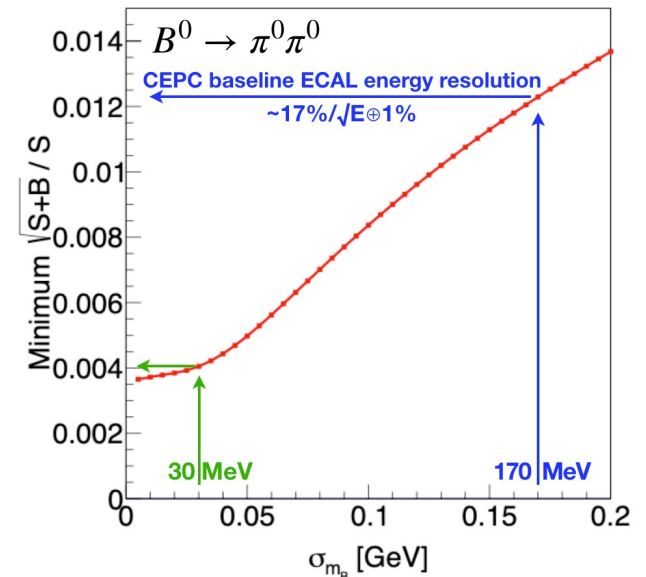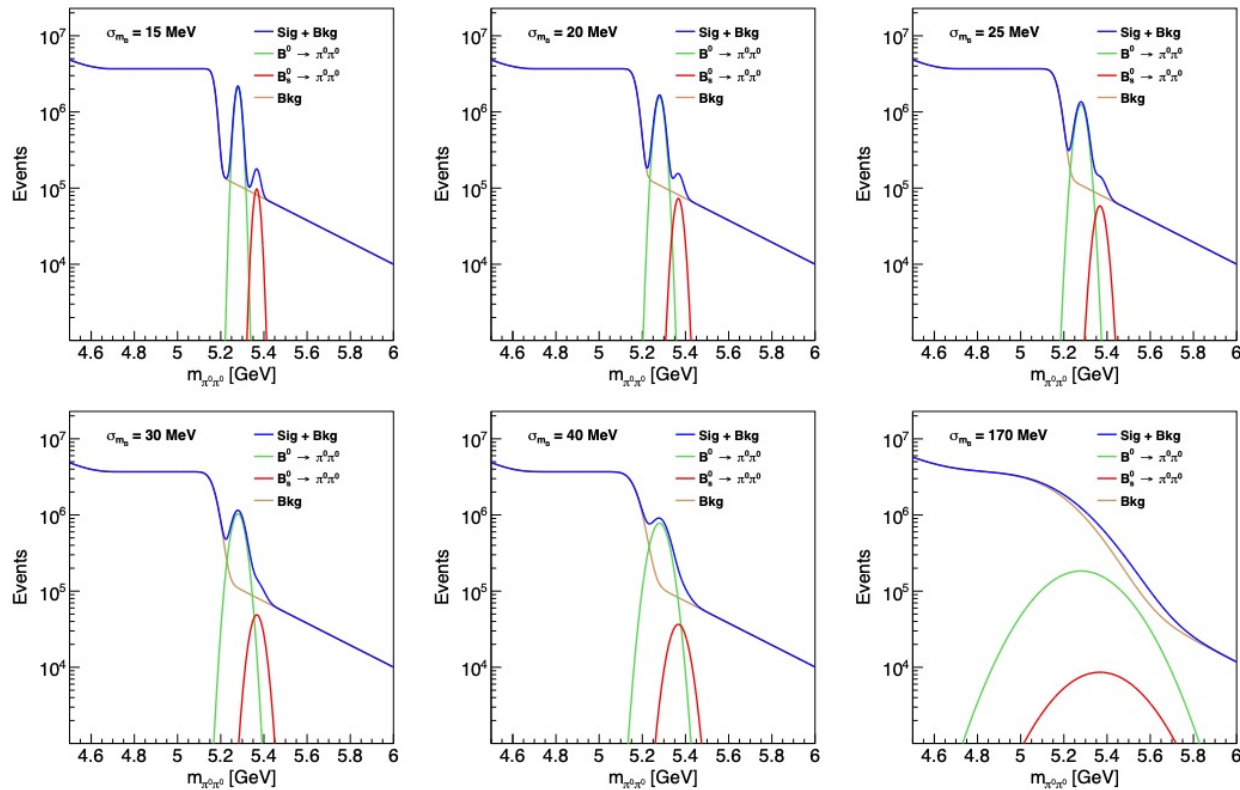>> $> 90\%$ for $E_{\pi^0} > 10$ GeV
>> $> 60\%$ for $E_\eta > 10$ GeV
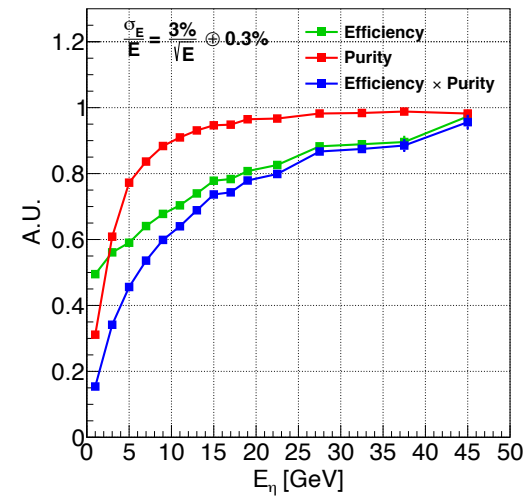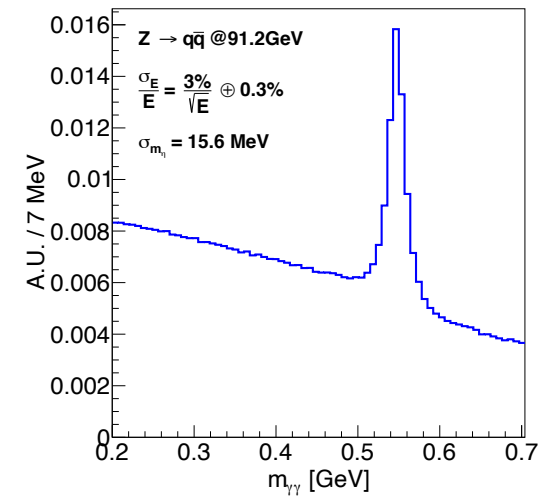
Background components of $B^0_{(s)} \to \pi^0\pi^0$

> Step structure mainly from $B^\pm \to X \to \pi^\pm\pi^0\pi^0$
>> $m^2_{\pi^0\pi^0} > 20 \text{ GeV}^2$
>>> $\sim 93\% \; B^\pm \to \rho(770)^\pm\pi^0, \rho(770)^\pm \to \pi^\pm\pi^0$
>>> $\sim 7\% \; B^\pm \to \pi^\pm\pi^0\pi^0$
> Kinematic constraint $\to$ cut-off on $m_{\pi^0\pi^0} \sim 5.2 \text{ GeV}$

Dependence on ECAL performance

➤ Using CEPC baseline b-tagging preformance

➤ ECAL performance is characterized by B mass resolution (σ_{m_B})

ECAL Resolution	σ_{m_B} (MeV)	$B^0 \to \pi^0\pi^0$	$B_s^0 \to \pi^0\pi^0$
$17\%/\sqrt{E} \oplus 1\%$	170	$\sim 1.2\%$	$\sim 21\%$
$3\%/\sqrt{E} \oplus 0.3\%$	30	$\sim 0.4\%$	$\sim 4\%$

3 ~ 5 times improvement

Estimation of other two $B \to \pi\pi$ modes

- $B^0 \to \pi^+\pi^-$ (MCTruth analysis)
  - E_tarck > 1 GeV
  - E_total > 20 GeV
  - $\theta < 30°$
  - |Vertex - IP| < 100 μm
  - Track momentum resolution ~0.1%
- $B^+ \to \pi^+\pi^0$ (Just a guesswork)
  - Anticipated performance in between 00 and +-
  - Rough estimation using "efficiency & purity"

$$\frac{\sigma_{\mathcal{B}}}{\mathcal{B}} \simeq \frac{1}{\sqrt{N_{\text{eff}}}} \equiv \frac{1}{\sqrt{\text{Yield} \times \epsilon \times p}}$$
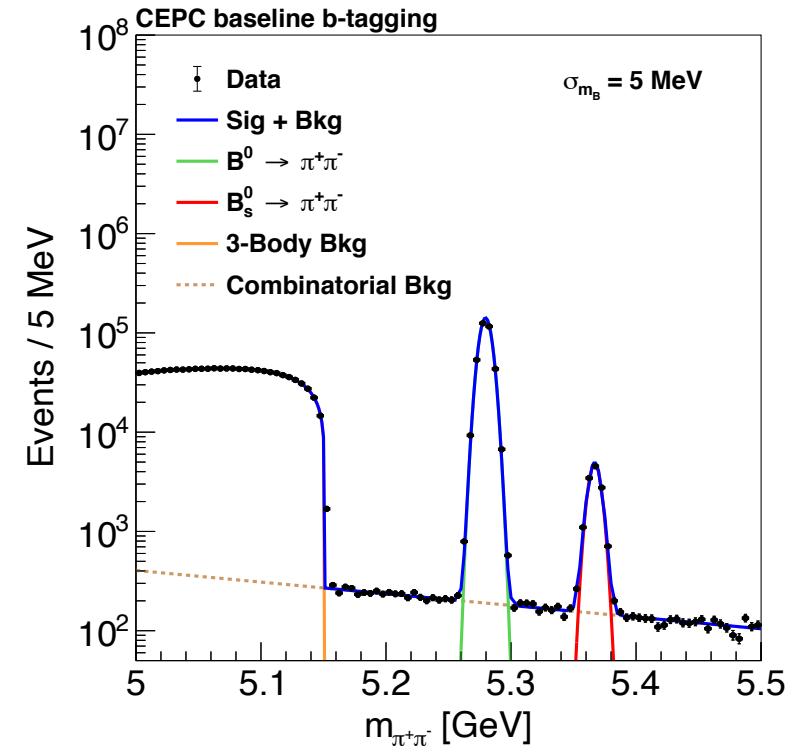
Channel	Branching ratio $\mathcal{B}$ ($\times 10^{-6}$)	Yield at Tera-Z	Efficiency ϵ	Purity p	$\epsilon \times p$	$\sigma_{\mathcal{B}}/\mathcal{B}$
$B^0 \to \pi^0\pi^0$	1.59	1.9×10^5	32%	80%	25%	0.45%
$B^+ \to \pi^+\pi^0$	5.50	6.6×10^5	50%	$\gtrsim 85\%$	43%	0.19%
$B^0 \to \pi^+\pi^-$	5.12	6.1×10^5	55%	$\gtrsim 95\%$	52%	0.18%

CP asymmetries of $B \to \pi\pi$

➢ Uncertainty estimation (only statistical)

$$\sigma_{a_{CP}^{00}} \simeq \frac{1}{(1 - 2\chi_d)\sqrt{N_{\text{eff}} \times \epsilon_{\text{eff}}}} \quad \text{(time-integrated)}$$

$$\sigma_{S_{CP}^{+-}} \simeq \sigma_{C_{CP}^{+-}} \simeq \frac{1}{\sqrt{N_{\text{eff}} \times \epsilon_{\text{eff}}}} \quad \text{(time-dependent)}$$

Parameters	Tera-Z Projection
$\sigma_{\mathcal{B}^{00}}/\mathcal{B}^{00}$	0.45%
$\sigma_{\mathcal{B}^{+0}}/\mathcal{B}^{+0}$	0.19%
$\sigma_{\mathcal{B}^{+-}}/\mathcal{B}^{+-}$	0.18%
$\sigma_{a_{CP}^{00}}$	$\pm (0.014 - 0.018)$
$\sigma_{C_{CP}^{+-}}$	$\pm (0.004 - 0.005)$
$\sigma_{S_{CP}^{+-}}$	$\pm (0.004 - 0.005)$

➢ b-charge tagging (B^0 or $\bar{B}^0$):
  ➢ effective tagging efficiency (power), ϵ_{eff}
    ➢ $\epsilon_{eff} \equiv \epsilon_{tag}(1 - 2\omega)^2 \in [15,25]\%$
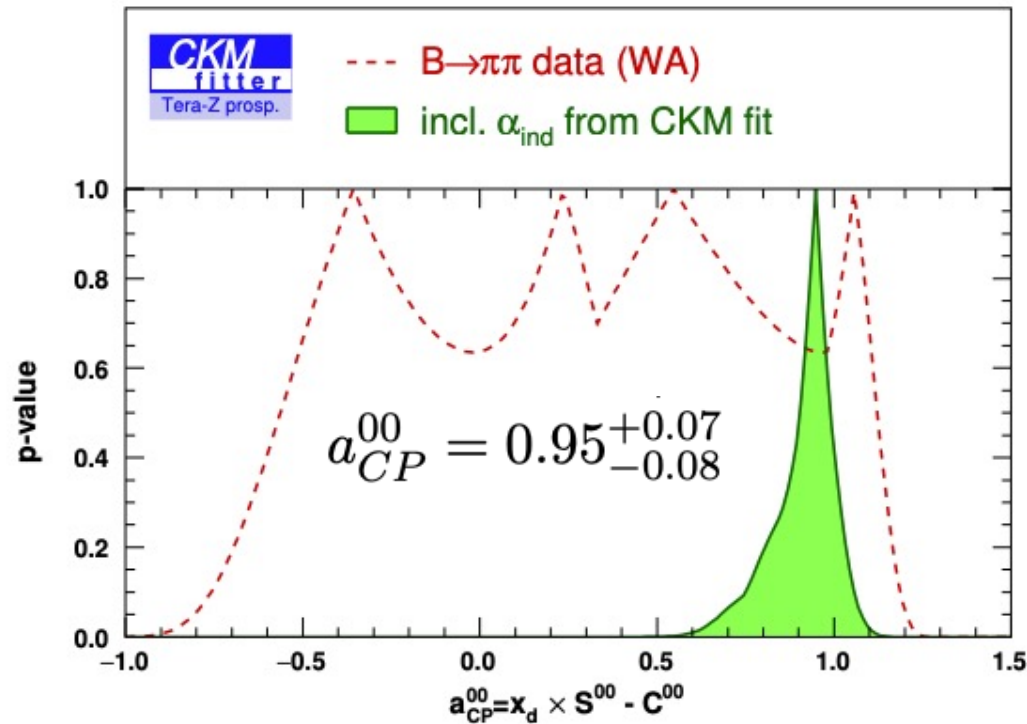   ➢ tagging efficiency, ϵ_{tag}
    ➢ wrong tag fraction, ω

➢ B^0-$\bar{B}^0$ mixing: $\chi_d = 0.1858 \pm 0.0011$

CKM global fit

by Sébastien & Olivier (CKMfitter group)

➢ Uncertainties rescaled to the Tera-Z projections
➢ The choice of central value
   ➢ a_{CP}^{00} and S_{CP}^{00}, current predictions of the CKM global fit
   ➢ Others, keep to the W.A.
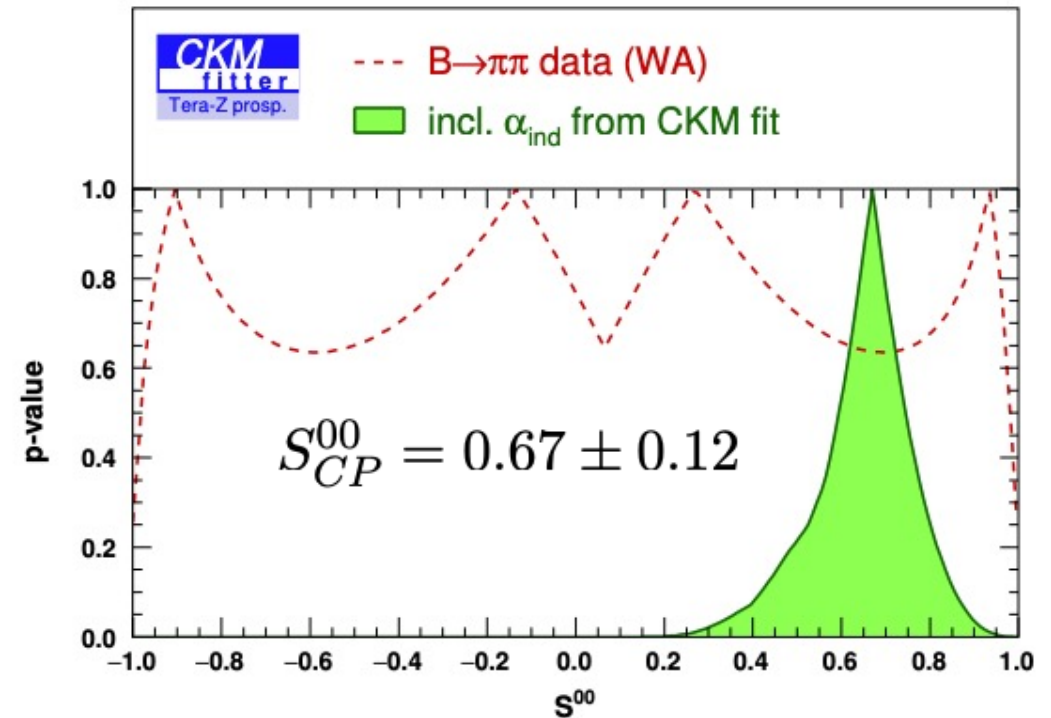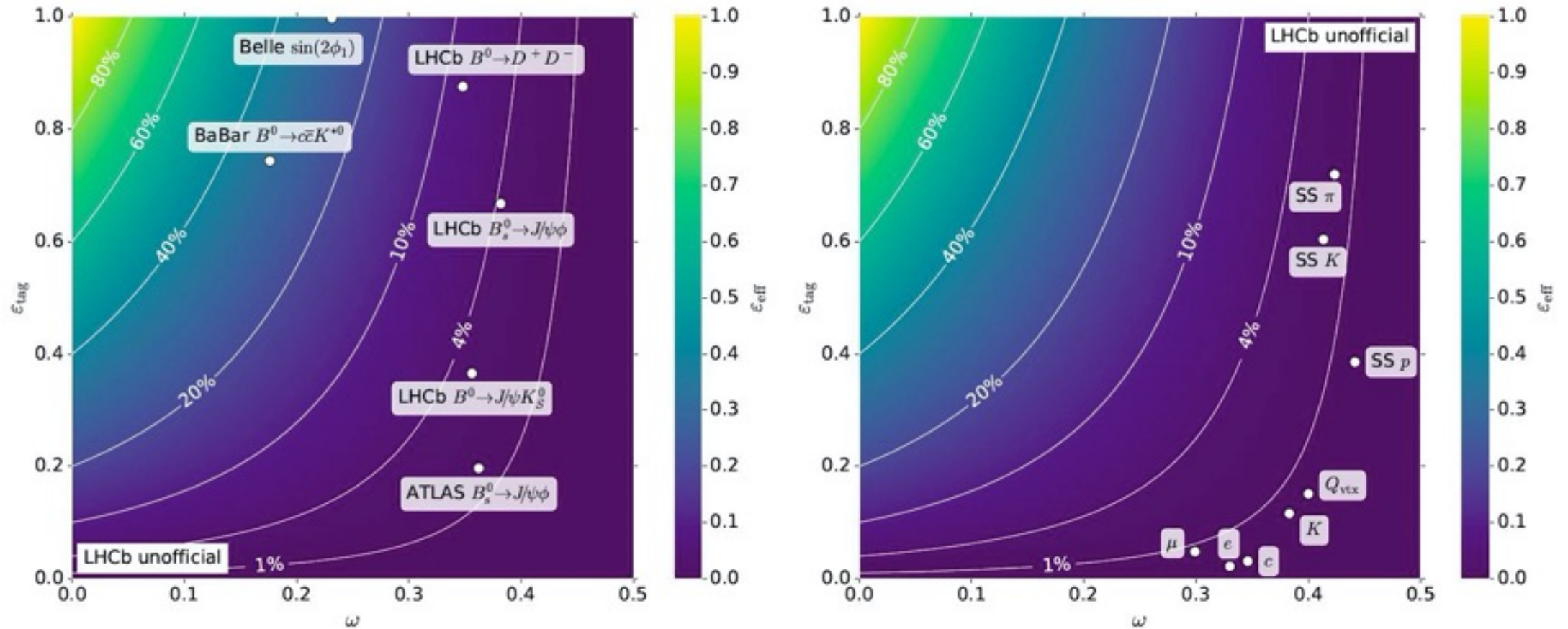
b-charge tagging (jet charge measurement)

Figure 3.1: Effective tagging efficiency of (left) different HEP experiments and (right) LHCb flavour tagging algorithms [40]. The white lines indicate contours of constant tagging power.

b-charge tagging (jet charge measurement)

- ➢ b-charge tagging performance:
  - ➢ wrong tag fraction, ω
  - ➢ tagging efficiency, ϵ_{tag}
  - ➢ effective tagging efficiency (power), ϵ_{eff}

$$\epsilon_{eff} = \epsilon_{tag}(1 - 2\omega)^2$$

- ➢ b-charge tagging at CEPC
  - ➢ Jet charge measurement at MCTruth level (by Hanhua)
    - ➢ infer b-charge by leading charged particles
    - ➢ $\omega \sim 35\%$, $\epsilon_{eff} \sim 10\%$
  - ➢ Dedicated b-charge tagging algorithm for $B_s \rightarrow J/\psi\phi$ (by Mingrui)
    - ➢ potential to improve $\omega \sim 25\%$, $\epsilon_{eff} \sim 20\%$

$$A_{CP}^{Measured} = \frac{[\bar{N}(1-\omega) + N\omega] - [\bar{N}\omega + N(1-\omega)]}{\bar{N} + N}$$
$$= (1 - 2\omega)\frac{\bar{N} - N}{\bar{N} + N} = (1 - 2\omega)A_{CP}^{Truth}$$

Time-dependent CP asymmetry of $B^0 \to \pi^0\pi^0$: $S_{\pi\pi}^{00}$

➤ Extra constraint of $S_{\pi\pi}^{00}$ can reduce the two-fold ambiguity on the solutions of α in [75, 105]°
➤ Time-dependent analysis need vertex information
  ➤ $\pi^0 \to e^+e^-\gamma$ Dalitz decay or photon conversion events
  ➤ Belle II: 147 Dalitz events & 124 photon conversion events
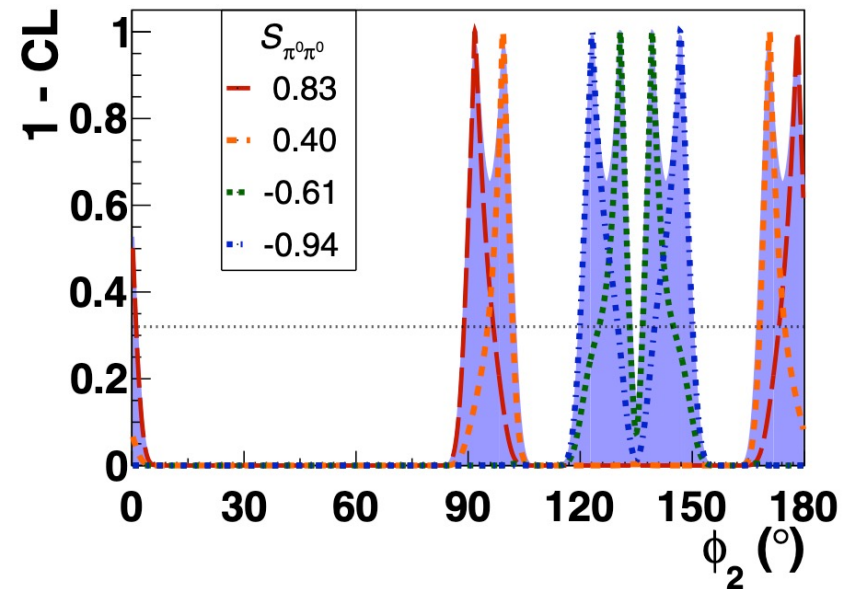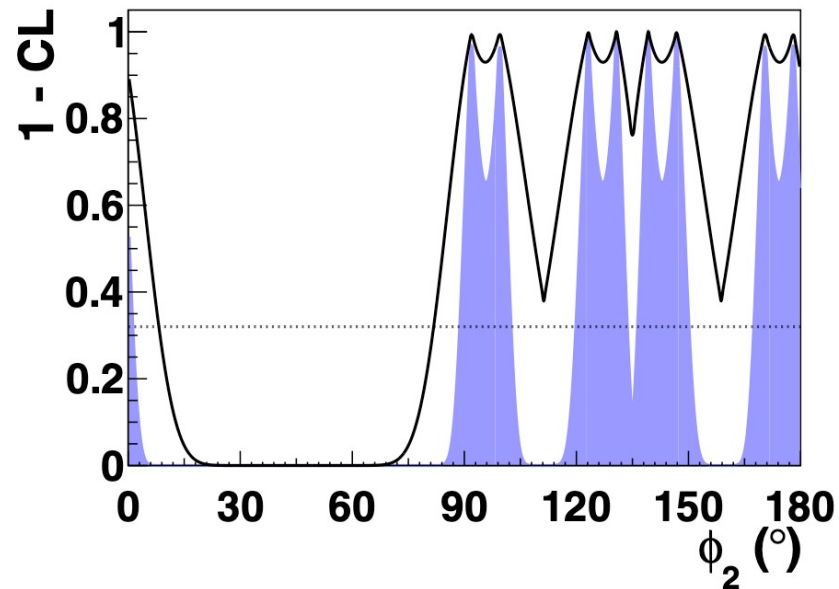
➤ CEPC advantage
  ➤ Larger boost of B meson
  ➤ Decent vertex reconstruction
  ➤ B decay lifetime resolution ~ 15 fs

More precise determination of α using $B \to \rho \, \rho$

- ➤ More precise than $B \to \pi \, \pi$ modes
  - ➤ Larger branching ratios than $B \to \pi \, \pi$
  - ➤ $B^0 \to \rho^0 \rho^0$ enjoys the charged final state $\rho^0 \to \pi^+ \pi^-$
    - ➤ Much better charged particle reconstruction performance than neutral particle
    - ➤ $S_{\rho\rho}^{00}$ is accessible to reduce the ambiguity solutions
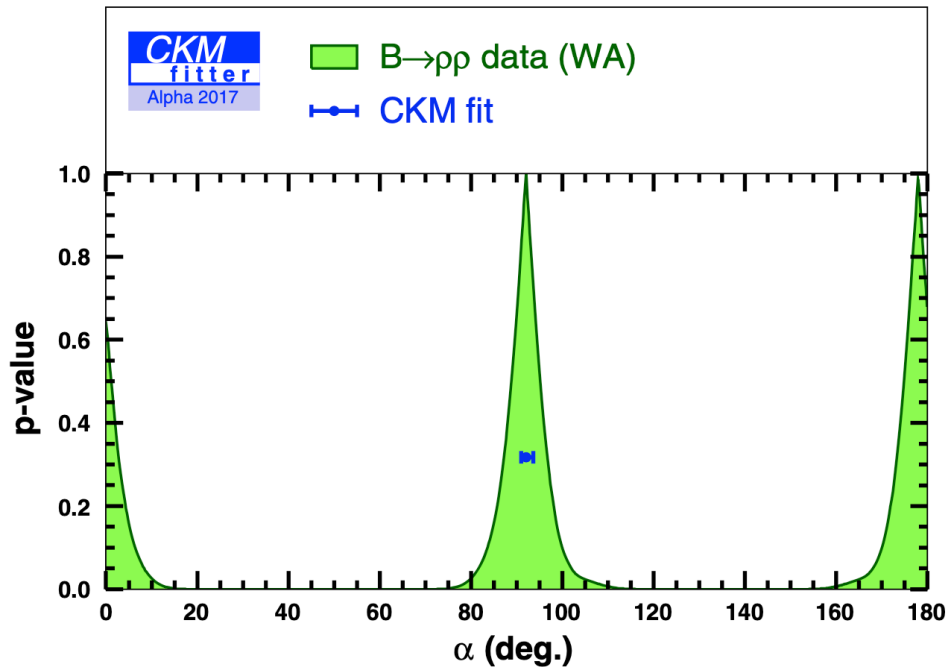

Table 4 World averages for the relevant experimental observables in the $B \to \rho^i \rho^j$ modes: branching fraction $\mathcal{B}_{\rho\rho}^{ij}$, fraction of longitudinal polarisation f_L^{ij}, time-integrated CP asymmetry $\mathcal{C}_{\rho\rho}^{ij}$, time-dependent asymmetry $\mathcal{S}_{\rho\rho}^{ij}$ and correlation (ρ)

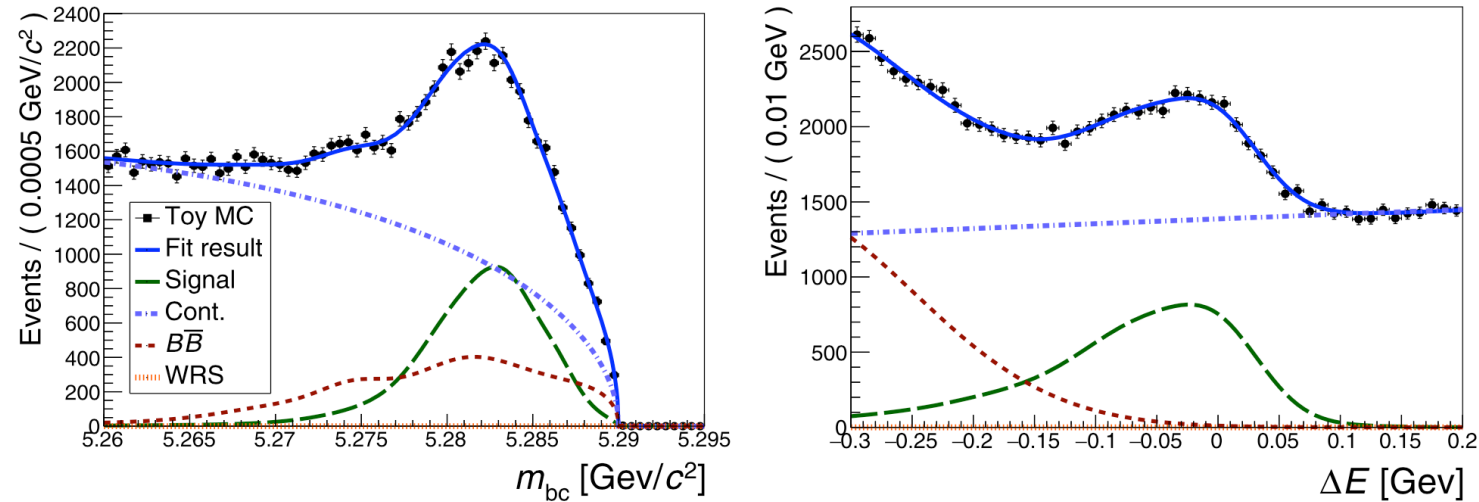| Observable	World average
$\mathcal{B}_{\rho\rho}^{+-} \times f_L^{+-} \ (\times 10^6)$	$(27.76 \pm 1.84) \times (0.990 \pm 0.020)$
$\mathcal{B}_{\rho\rho}^{+0} \times f_L^{+0} \ (\times 10^6)$	$(24.9 \pm 1.9) \times (0.950 \pm 0.016)$
$\mathcal{B}_{\rho\rho}^{00} \times f_L^{00} \ (\times 10^6)$	$(0.93 \pm 0.14) \times (0.71 \pm 0.06)$
$\mathcal{C}_{\rho_L\rho_L}^{+-}$	-0.00 ± 0.09
$\mathcal{S}_{\rho_L\rho_L}^{+-}$	-0.15 ± 0.13
$\rho(C_{\rho_L\rho_L}^{+-}, S_{\rho_L\rho_L}^{+-})$	$+0.0002$
$\mathcal{C}_{\rho_L\rho_L}^{00}$	0.2 ± 0.9
$\mathcal{S}_{\rho_L\rho_L}^{00}$	0.3 ± 0.7

Belle II

Fig. 113. Projections of the fit results for candidates reconstructed as $B^0 \rightarrow \pi^0(\rightarrow \gamma\gamma)\pi^0(\rightarrow \gamma\gamma)$. The projections for one example pseudo-experiment are shown onto $M_{\rm bc}$ (left) and ΔE (right). Points with error bars represent the toy sample. The full fit results are shown by the solid blue curves. Contributions from signal, generic $B\bar{B}$ events, continuum background, and background from wrongly reconstructed signal events are shown by the long dashed green, short dashed red, dash-dotted blue, and dotted orange curves, respectively. The input values used for this pseudo-experiment are $A_{\pi^0\pi^0} = 0.34$ and $S_{\pi^0\pi^0} = 0.65$.

$B\bar{B}$ background   Sources of background from $B\bar{B}$ events are studied with a 4 ab^{-1} MC sample. The largest contribution comes from $B^+ \rightarrow \rho^+(\rightarrow \pi^+\pi^0)\pi^0$ decays, where the π^+ is lost. Events where the remaining π^0 pair decays into four photons which arrive at the ECL are the main $B\bar{B}$ background for $B^0 \rightarrow \pi^0_{\gamma\gamma}\pi^0_{\gamma\gamma}$ candidates. Those events which contain a converted photon or a Dalitz π^0 are the main background $B\bar{B}$ source for $B^0 \rightarrow \pi^0_{\rm dal}\pi^0_{\gamma\gamma}$ candidates. This background peaks at the same value of $M_{\rm bc}$, but is shifted in ΔE towards negative values due to the missing π^+.

Table 90. Statistical uncertainties $\Delta A_{\pi^0\pi^0}$, $\Delta S_{\pi^0\pi^0}$, and $\Delta \mathcal{B}_{\pi^0\pi^0}/\mathcal{B}_{\pi^0\pi^0}$ for different input values of $A_{\pi^0\pi^0}$ and $S_{\pi^0\pi^0}$ used for the generation of signal MC.

Input values		Time-dependent		Time-integrated	
$A_{\pi^0\pi^0}$	$S_{\pi^0\pi^0}$	$\Delta A_{\pi^0\pi^0}$	$\Delta S_{\pi^0\pi^0}$	$\Delta A_{\pi^0\pi^0}$	$\Delta \mathcal{B}_{\pi^0\pi^0}/\mathcal{B}_{\pi^0\pi^0}$ [%]
0.34 [650]	0.65 [650]	0.22	0.28	0.03	2.2
0.43 [88]	0.79	0.23	0.29	0.03	2.2
0.14 [712]	0.83	0.21	0.26	0.03	2.4
0.14 [712]	0.40	0.20	0.29	0.03	2.3
0.14 [712]	−0.61	0.22	0.27	0.03	2.3
0.14 [712]	−0.94	0.22	0.28	0.03	2.4

Table 91. Branching fractions and CP asymmetry parameters entering in the isospin analysis of the $B \to \pi\pi$ system: Belle measurements at $0.8\,\text{ab}^{-1}$ together with the expected Belle II sensitivity at $50\,\text{ab}^{-1}$.

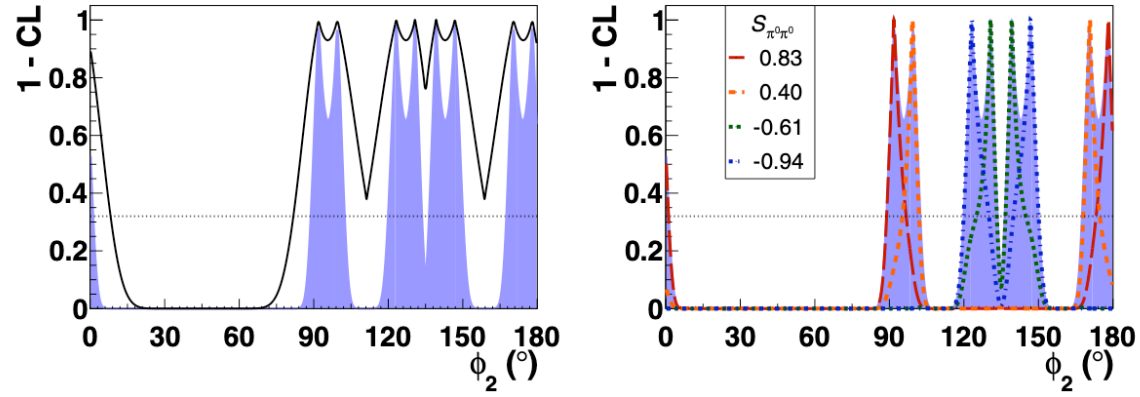|	Value	$0.8\,\text{ab}^{-1}$	$50\,\text{ab}^{-1}$
$\mathcal{B}_{\pi^+\pi^-}$ [10^{-6}]	5.04	$\pm 0.21 \pm 0.18$ [727]	$\pm 0.03 \pm 0.08$
$\mathcal{B}_{\pi^0\pi^0}$ [10^{-6}]	1.31	$\pm 0.19 \pm 0.19$ [712]	$\pm 0.03 \pm 0.03$
$\mathcal{B}_{\pi^+\pi^0}$ [10^{-6}]	5.86	$\pm 0.26 \pm 0.38$ [727]	$\pm 0.03 \pm 0.09$
$A_{\pi^+\pi^-}$	0.33	$\pm 0.06 \pm 0.03$ [728]	$\pm 0.01 \pm 0.03$
$S_{\pi^+\pi^-}$	−0.64	$\pm 0.08 \pm 0.03$ [728]	$\pm 0.01 \pm 0.01$
$A_{\pi^0\pi^0}$	0.14	$\pm 0.36 \pm 0.10$ [712]	$\pm 0.03 \pm 0.01$

Fig. 116. Scan of the confidence for ϕ_2 performing isospin analysis of the $B \to \pi\pi$ system. (Left): The black solid line shows the result of the scan using data from Belle measurements (see Table 91). The blue shaded area in both plots shows the projection for Belle II. (Right): Results of the scan adding the $S_{\pi^0\pi^0}$ constraint. Each line shows the result for a different $S_{\pi^0\pi^0}$ value. The dotted horizontal lines correspond to 1σ.
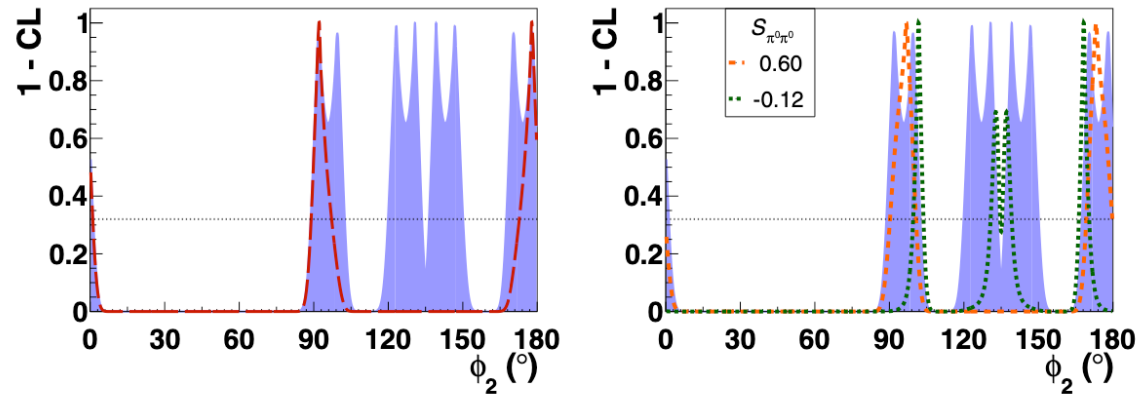

Fig. 117. Scan of the confidence for ϕ_2 performing isospin analysis of the $B \to \pi\pi$ system. The blue shaded area in both plots shows the projection of the Belle measurements (see Fig. 116) for Belle II. Results of the scan with additional $S_{\pi^0\pi^0}$ constraints are shown by dashed lines. Each line correspond to different input $S_{\pi^0\pi^0}$ values. The red long dashed line on the left figure shows the result for $S_{\pi^0\pi^0} = 0.83$. The dotted horizontal line correspond to 1σ.

$B^0 \to \pi^0\pi^0$	Final state	Total in theory	In acceptance	Selected	Efficiency	Purity	Relative accuracy
Tera-Z	$\pi\pi$	195692	-	-	-	-	-
	$\pi_{\gamma\gamma}\pi_{\gamma\gamma}$	191113*0.65 = 124223	-	75859 49689	0.4	0.8 0.72	0.4% 0.5%
	$\pi_{dal}\pi_{\gamma\gamma}$	4579	-	?	?		
	$\pi_{\gamma c\gamma}\pi_{\gamma\gamma}$	191113*0.2 = 38222	-	?	?		
Belle II	$\pi\pi$	103000	-	-	-	-	-
	$\pi_{\gamma\gamma}\pi_{\gamma\gamma}$	100590 - 9270 = 91320	78486	15068	0.192	0.158	2%
	$\pi_{dal}\pi_{\gamma\gamma}$	2410	2060	147	0.072	0.176	
	$\pi_{\gamma c\gamma}\pi_{\gamma\gamma}$	100590*0.09 = 9270	3090	124	0.042		

$\pi^0_{\gamma\gamma}$ are used for the time-integrated CP violation study. There is no event overlap between events with B^0_{sig} candidates reconstructed from two $\pi^0_{\gamma\gamma}$ and events containing Dalitz decays or converted photons.
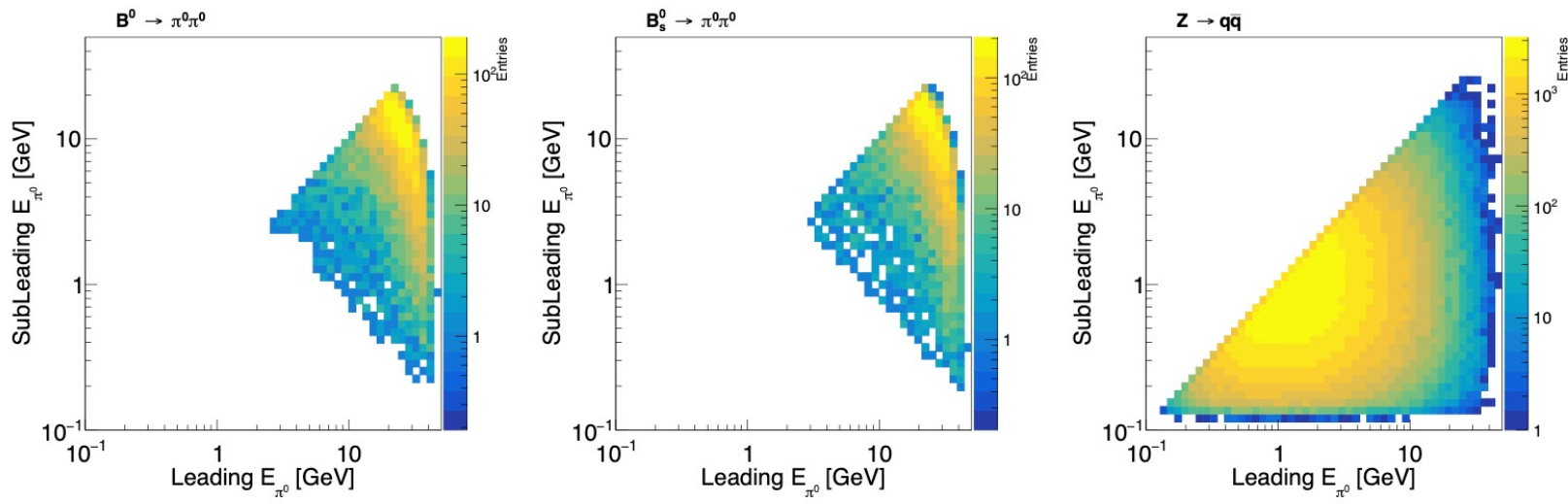
(a) 2D energy spectrum of π^0 pairs in $B^0 \to \pi^0\pi^0$ (left), $B_s^0 \to \pi^0\pi^0$ (middle), and $Z \to q\bar{q}$ (right) events.
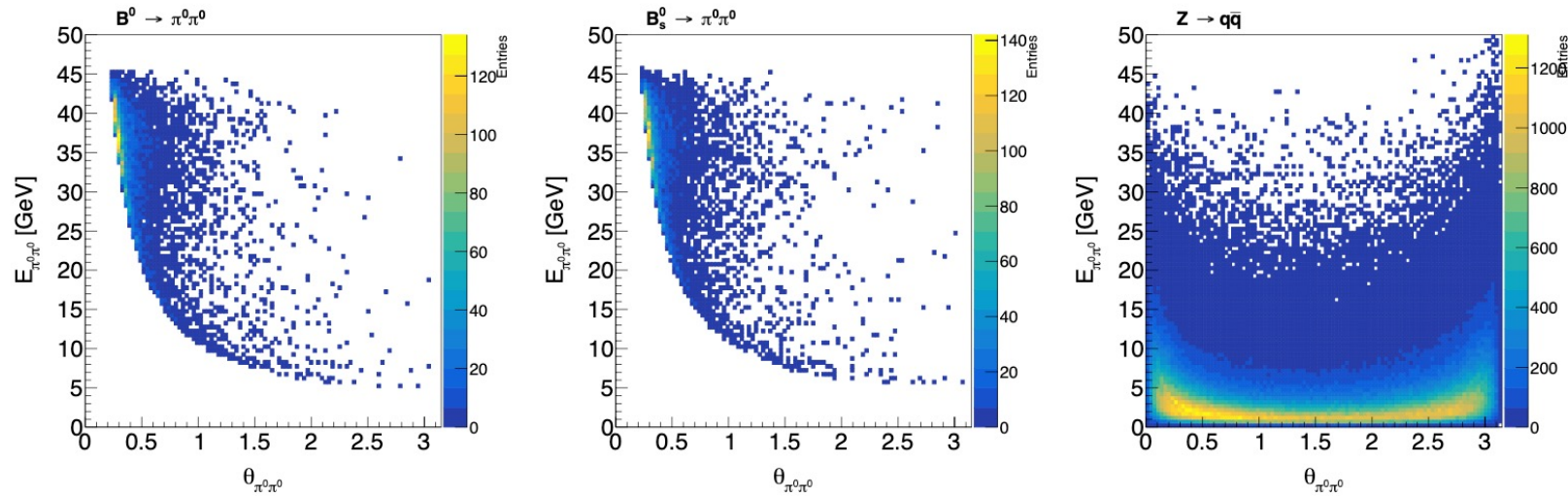
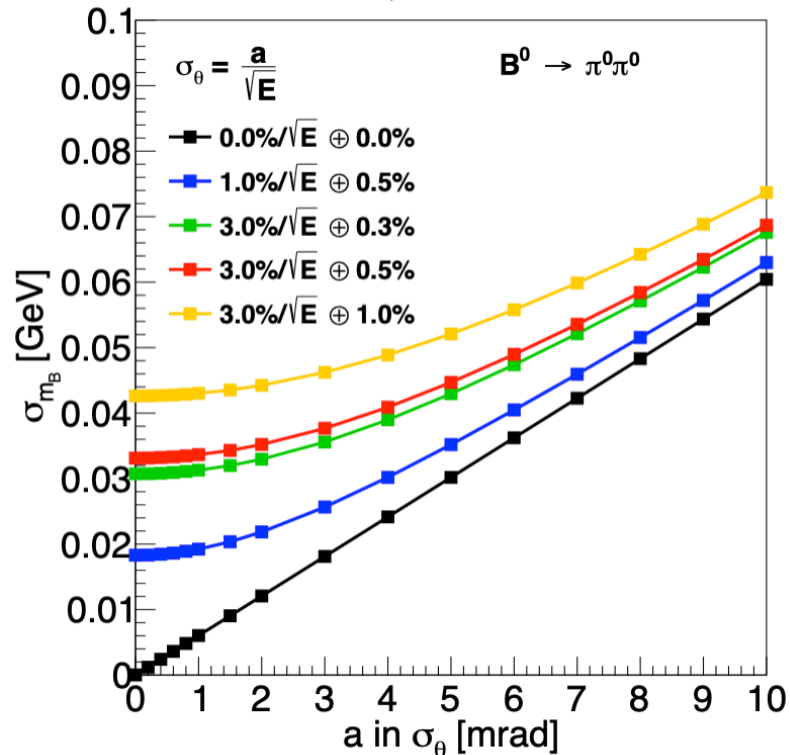(b) Correlation between $E_{\pi^0\pi^0}$ and $\theta_{\pi^0\pi^0}$ in $B^0 \to \pi^0\pi^0$ (left), $B_s^0 \to \pi^0\pi^0$ (middle), and $Z \to q\bar{q}$ (right) events.

Dependence of B mass resolution on detector performance

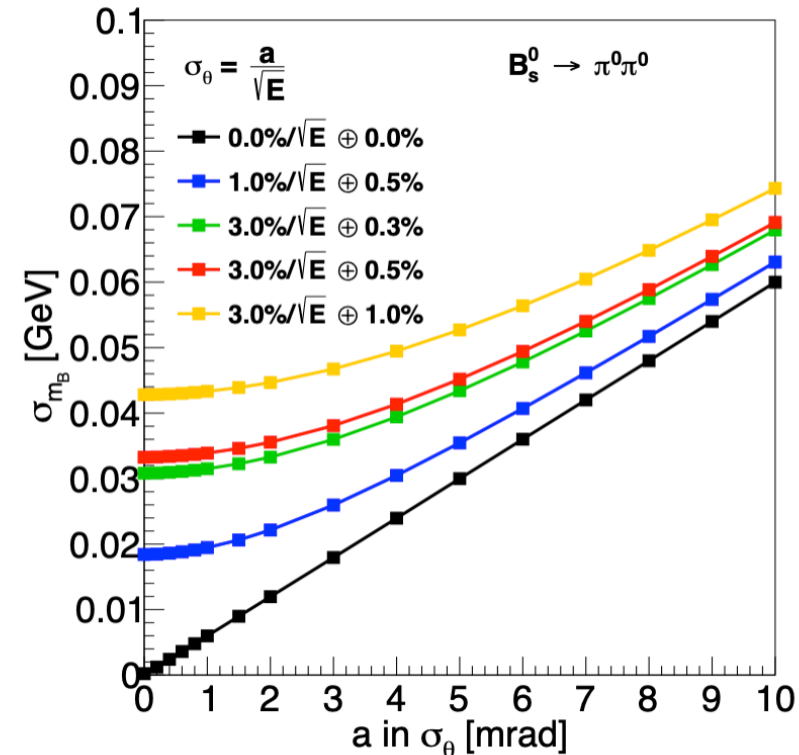**ECAL energy resolution**

$$\frac{\sigma_E}{E} = \frac{A}{\sqrt{E}} \oplus C$$

Photon angular resolution

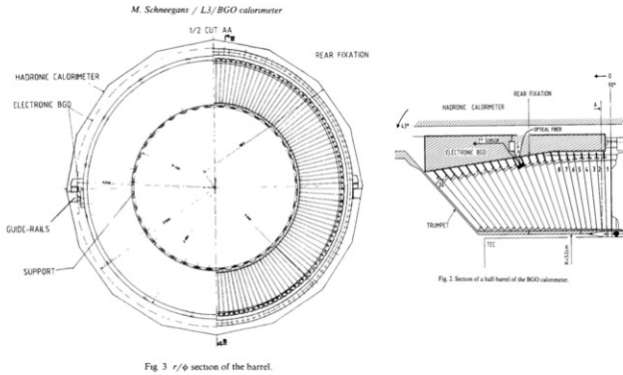$$\sigma_\theta = \frac{a}{\sqrt{E}}, \; \sigma_\phi = \frac{\sigma_\theta}{sin\theta}$$

- CEPC baseline single photon angular resolution ~1mrad/√E
- ECAL energy resolution dominates the contribution when σ_θ < 1mrad/√E
- The following analysis only takes ECAL energy resolution into account
- σ_{mB} ~30 MeV requires ECAL energy resolution ~3%/√E⊕0.3%

EM Energy Resolution

From a historical perspective

LEP - L3, BGO

LHC - CMS, PbWO4

DAMPE, BGO
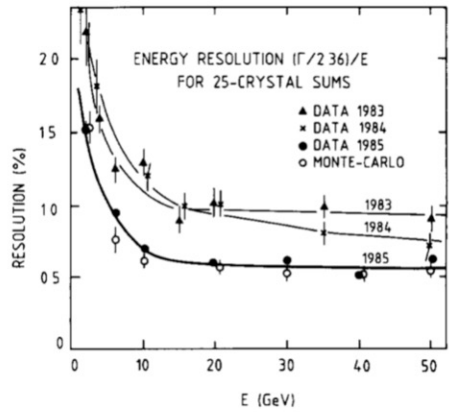
< 2% at 1GeV

$2.8\%/\sqrt{E} \oplus 0.3\%$

$5.86\%/\sqrt{E} \oplus 0.78\%$
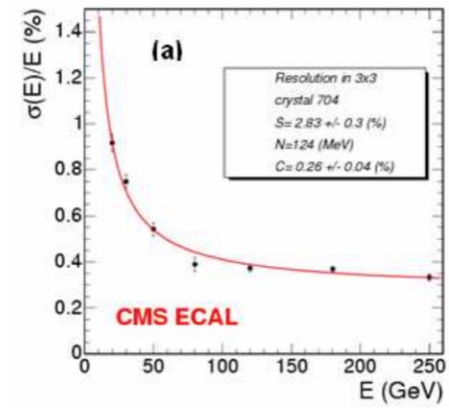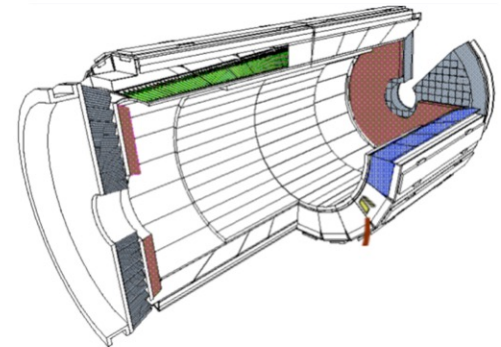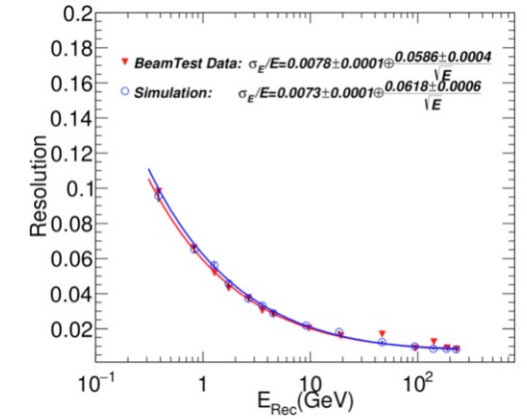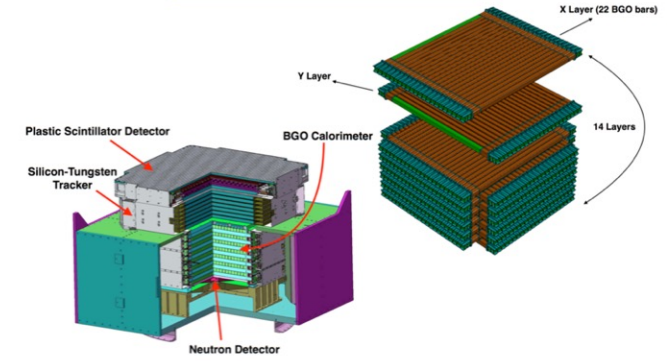
The performance now measured in electron beams
with final prototypes shows that we are below 2%
energy resolution at 1 GeV and near to 5% at 100 MeV.

Belle II ECAL

The intrisic energy resolution of the calorimeter, as measured in a prototype [3], can be approximated as:

$$\frac{\sigma_E}{E} = \sqrt{\left(\frac{0.066\%}{E}\right)^2 + \left(\frac{0.81\%}{\sqrt[4]{E}}\right)^2 + (1.34\%)^2}, \qquad (9.1)$$

where E is in GeV and the first term represents the electronics noise contribution.

3.5. Electromagnetic calorimeter (ECL)

The electromagnetic calorimeter is used to detect gamma rays as well as to identify electrons, i.e. separate electrons from hadrons, in particular pions. It is a highly segmented array of thallium-doped caesium iodide CsI(Tl) crystals assembled in a projective geometry (Fig. 3). All three detector regions, the barrel as well as the forward and backward endcaps, are instrumented with a total of 8736 crystals, covering about 90% of the solid angle in the centre-of-mass system. The CsI(Tl) crystals, preamplifiers, and support structures have been reused from Belle, whereas the readout electronics and reconstruction software have been upgraded. In the Belle experiment, the energy resolution observed with the same calorimeter was $\sigma_E/E = 4\%$ at 100 MeV, 1.6% at 8 GeV, and the angular resolution was 13 mrad (3 mrad) at low (high) energies; π^0 mass resolution was 4.5 MeV/c^2 [2]; in the absence of background a very similar performance would also be expected for Belle II.